Přírodovědecká fakulta
Faculty of Science

Jihočeská univerzita v Českých Budějovicích
University of South Bohemia in České Budějovice

Post-transcriptional regulation of $TbIF_1$ in life cycle of *Trypanosoma brucei*

Bachelor's thesis

Sascha Gratzl

2020

České Budějovice
Supervisor: Mgr. Ondřej Gahura, PhD

Gratzl, S., 2020: Post-transcriptional regulation of $TbIF_1$ in life cycle of *Trypanosoma brucei*. Bc. Thesis, in English – 51 p., Faculty of Science, University of South Bohemia, České Budějovice, Czech Republic

Annotation:
$TbIF_1$, a protein Inhibitor of F_1-ATPase in *Trypanosoma brucei*, is expressed exclusively in the insect stage of the parasite. In the bloodstream form, $TbIF_1$ is switched off, because its activity interferes with the essential role of the ATP synthase in the maintenance of the mitochondrial membrane potential. Here, we employ a series of reporter genes to study the impact of 3'UTR of $TbIF_1$ on mRNA stability and translatability to get insight into the tight post-transcriptional control of $TbIF_1$. We provide evidence that developmentally regulated RNA binding protein Rbp10 is critical for downregulation of $TbIF_1$ on translation level in bloodstream-form trypanosomes.

I hereby declare that I have worked on my bachelor's thesis independently and used only the sources listed in the bibliography.

I hereby declare that, in accordance with Article 47b of Act No. 111/1998 in the valid wording, I agree with the publication of my bachelor thesis, in full form to be kept in the Faculty of Science archive, in electronic form in publicly accessible part of the STAG database operated by the University of South Bohemia in České Budějovice accessible through its web pages.

Further, I agree to the electronic publication of the comments of my supervisor and thesis opponents and the record of the proceedings and results of the thesis defense in accordance with aforementioned Act No. 111/1998. I also agree to the comparison of the text of my thesis with the Theses.cz thesis database operated by the National Registry of University Theses and a plagiarism detection system.

……17. 5. 2020….. ……

Dobersberg Sascha Gratzl

Acknowledgment

I would like to thank Alena for giving me the opportunity to work in her lab. But special thanks are directed to Ondra. Thank you so much - for all the time and effort you invested into me, for your perseverance and encouraging words when things were difficult, for teaching me skills and scientific thinking, and thank you so much for introducing me into the world of science. Every former and future student who worked and will work with you, can be delighted and grateful to call you his/her supervisor.

Contents

1. Introduction

1.1. The parasite *Trypanosoma brucei* and its life cycle

The protozoan parasite *Trypanosoma brucei* is transmitted by the tsetse fly (genus *Glossina*) to mammalian hosts and can infect cattle as well as humans. In humans an infection can result in human African trypanosomiasis (HAT) or sleeping sickness. The highly deadly disease is decreasing globally (6000 cases in 2013 [1]) but infections of livestock reduce the milk and meat production and therefore the animal African trypanosomiasis has a direct effect on the African economy and local food supply [2]. The parasite, which belongs to the supergroup of Excavates, diverged early from other eukaryotes (>600 Mio years) and has therefore a highly atypical metabolism [3]. Due to the fact, that it encounters different environments in its life cycle, massive metabolic and morphological changes are crucial and depend on specific gene expression regulation [4]. Different adaptations include for example the switch from a proline-rich environment in the tsetse fly [5] to glucose as the preferred nutrient in the mammalian host [6] (Fig. 1.). Therefore, the main path for ATP production changes from oxidative phosphorylation (OXPHOS) to glycolysis in the life cycle of trypanosomes [4]. In mammals the parasite also encounters the immune defense system [7] rather than proteolytic protective mechanisms found in the insect vector [8]. *T. brucei* has therefore a gene expression regulation system controlling specific genes expressed either in the mammalian host or the vector. These adaptations are mandatory to face the diverse molecular environments in e.g. tsetse fly salivary glands or mammalian blood [4].

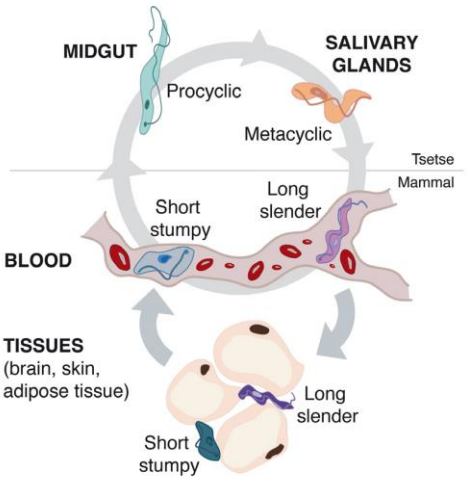

Tsetse - midgut	Procyclic form (PF)
Preferred nutrient	Proline (and glucose, if available)
Main secreted products	Alanine, (acetate and succinate)
Main pathways for ATP production	Oxidative phosphorylation (and glycolysis)
Respiratory chain	Active
Proliferation (Doubling Time)	~12 hr

Mammal - blood	Long slender (B-LS)	Short stumpy (B-SS)
Preferred nutrient	Glucose	Glucose
Main secreted products	Pyruvate	Pyruvate (Acetate and Succinate)
Main pathways for ATP production	Glycolysis	Glycolysis (and Oxidative Phosphoryation?)
Respiratory chain	Inactive (TAO maintains redox)	Probably Active
Proliferation (Doubling Time)	~7 hr	Quiescent

Figure 1: Metabolic and morphological changes in the life cycle of T. brucei. Adopted from [4]

1.2. Gene expression regulation in trypanosomatids

Gene expression in *T. brucei*, like in all other trypanosomatids, is not controlled by transcription initiation of single genes, because genes are transcribed as polycistronic units into primary transcripts containing multiple coding sequences [9]. The length of the primary transcripts can vary from several to 100 kb and the transcripts contain various, functionally unrelated, genes. The polycistronic transcripts are processed by trans-splicing [10] into individual mRNAs, 5' capped and 3'-polyadenylated [11]. Because trypanosomes lack an individual gene expression control on the transcription level, they widely use other regulation mechanisms on post-transcriptional level, like differential mRNA stability and translation efficiency. mRNA stability and therefore its abundance is predominantly controlled by deadenylation [12] (in case of the 3'-5' degradation) and decapping factors [13] (in 5'-3' degradation) mediated through sequences in the mRNA 3'-untranslated region (3'-UTR). These regions are often at least 100 nt long (the mean length of 3'UTRs in *T. brucei* is 400 nt) and harbor conserved motifs and secondary structure elements recognized by RNA binding proteins (Rbp). [14, 15, 9] Rbp's cannot only induce mRNA degradation or translation inhibition, but can act also as mRNA stabilizing factors, as the ELAV-Like protein 1, similar to human ELAV, which is involved in the regulation of procyclic specific genes like the glycosomal phosphoglycerate kinase [16].

1.3. Metabolic features of the F_1F_o-ATP-Synthase

T. brucei has a single mitochondrion with different morphology in procyclic and bloodstream stage form (BF). In the procyclic stage, it has a branched structure with discoid cristae but in BF it is less developed, having a narrow and tubular structure [4]. The stage-specific mitochondrial processes for energy production are depicted in figure 2. ATP and ADP molecules are interchanged between the mitochondrial matrix and the cytosol through a transmembrane ADP/ATP exchanger, called ATP/ADP carrier (AAC) or adenine nucleotide translocase [17]. This activity is crucial also in the BF because no OXPHOS is carried out in the BF and ATP is presumably imported to the organelle. For maintenance of the proton gradient and the electrochemical potential of the inner mitochondrial membrane, the F_1F_0-ATP-synthase (F_1F_0-ATPase) works in the reverse direction, hydrolyzing ATP and pumping protons to the intermembrane space. In BF all ATP is believed to be generated

through glycolysis, in contrast to the conversion of proline to alanine, which is the major ATP production path in procyclic form [4].

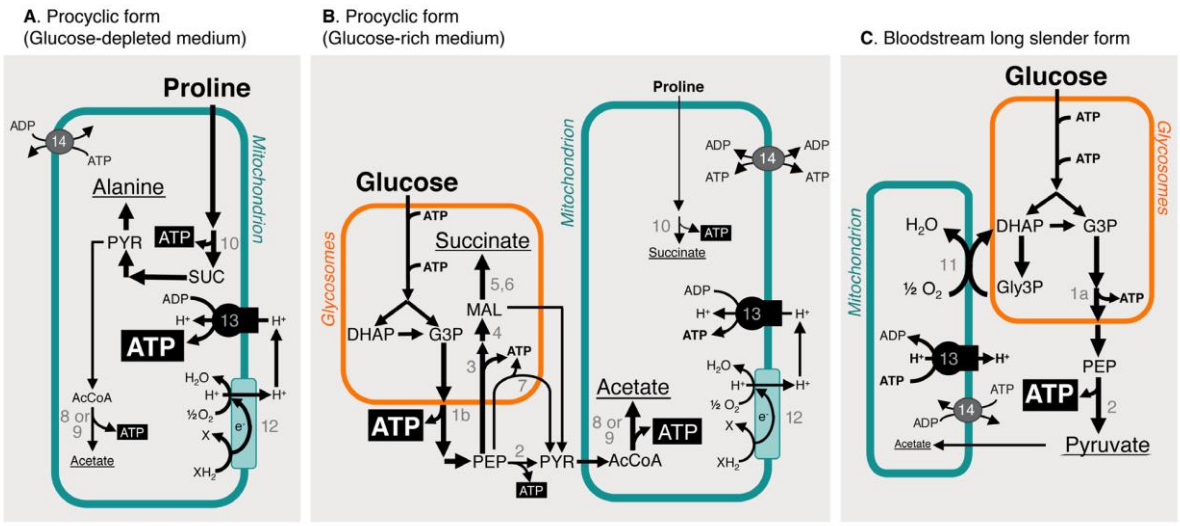

Figure 2: Different pathways for ATP production in T. brucei. Key steps: 1a: glycosomal phosphoglycerate kinase; 1b: cytosolic phosphoglycerate kinase; 2: pyruvate kinase; 3: phosphoenolpyruvate carboxykinase; 4: glycosomal malate dehydrogenase; 5: cytosolic fumarase; 6: glycosomal NADH-dependent fumarate reductase; 7: pyruvate phosphate dikinase; 8: acetate-succinate coenzyme A-transferase / ASCT; 9: acetyl-coenzyme A thioesterase; 10: succinyl-coenzyme A synthetase; 11: trypanosome alternative oxidase; 12: respiratory chain; 13: F0F1-ATP synthase; 14: mitochondrial ADP/ATP exchanger. AcCoA: acetyl-coenzyme A; DHAP: dihydroxyacetone phosphate; G3P: glyceraldehyde 3-phosphate; Gly3P: glycerol 3-phosphate; MAL: malate; PEP: phosphoenolpyruvate; PYR: pyruvate; SUC: succinate. Adopted from [4]

1.4. TbIF$_1$ and its differential expression in the life cycle

Typically, the reversed catalytic function of the F_1F_o-ATPase is only found in eukaryotes when sporadic hypoxic conditions lead to mitochondrial membrane depolarization, causing the hydrolysis of ATP to ADP [18]. To protect from the complete depletion of cellular ATP, a small protein known as inhibitory factor 1 or inhibitor of F_1-ATPase (IF_1) binds to the catalytic part of the F_1F_0-ATPase, resulting in an inhibition of the hydrolytic activity by interaction with the central stalk of the enzyme, disabling its rotation [19]. IF_1 inhibits the hydrolytic activity of the F_1F_0-ATPase, but it does not affect the synthetic function of the enzyme [20].

IF_1 is present in *T. brucei* (termed $TbIF_1$) but expressed only in the procyclic form (PF) [21]. Under normal conditions, the expression of $TbIF_1$ is switched off in BF, because the hydrolysis of ATP and proton pumping into the intermembrane space maintains the

mitochondrial membrane potential. Steady-state levels of $TbIF_1$ mRNA are about 5-times higher in PF than in BF (Fig. 3, O. Gahura, unpublished data) and translational efficiency is

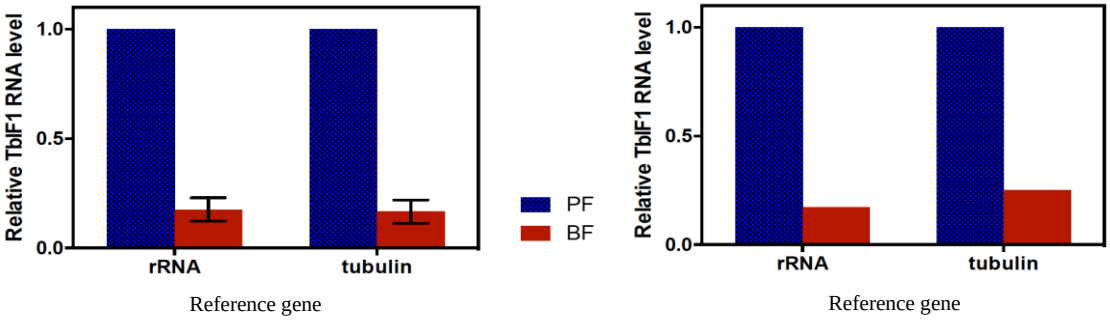

Figure 3: $TbIF_1$ mRNA steady state level in BF and PF detected by Northern Blot (left panel) and real time qualitative polymerase chain reaction (RT-qPCR; right panel). The values were normalized to 18s rRNA or tubulin levels.

lower in BF than in PF [22], suggesting post-transcriptional regulation on mRNA level. But this difference is not sufficient to explain the massive difference in protein level - $TbIF_1$ is not detectable in BF by immunoblotting with a specific antibody, but it shows a strong specific signal in PF [Fig 4, 21]. Induction of a very low expression level of $TbIF_1$ leads to cell death due to interference of the ATP hydrolyzing activity of the F_1F_0-ATPase and mitochondrial potential depletion in BF [21]. This unidirectional inhibitory function can be exploited in the future for the design of a drug inhibiting specifically the hydrolytic function in *T. brucei*, which is necessary for survival in BF, but not affecting the ATP producing activity in the host mammalian cells [23].

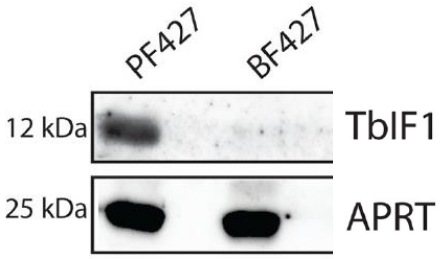

Figure 4: The levels of $TbIF_1$ in T. brucei PF427 and BF427 whole cell lysates analyzed by western blot with anti-$TbIF_1$ specific antibody. Signal of APRT (adenine phosphoribosyl transferase) was detected as a loading control. [21]

The 3'UTR of $TbIF_1$ transcript (see Figure 10 for a scheme; the full sequence can be found in Appendix 1) contains several regions with possible role in regulation. First, it contains two U-rich elements. U-rich elements have been shown to be involved in the negative regulation of PF-specific genes, namely tsetse-specific immune responsive protein EP, procyclic-specific cytosolic phosphorglycerate kinase (PGKP) and pyruvate, phosphate dikinase in BF, where the deletion of the motif lead to an increase of the respective mRNA half-lives from approximately 5 to 15-30 min [24]. Further, it contains two regions that are

predicted to form stem-loop structures with high probability (Fig. 5). Secondary structures can control expression [26] and are often recognized by regulatory RNA binding proteins. Finally, the 3'UTR sequence includes two UA(U)$_6$ motifs, which are overrepresented in 3'UTRs of PF-specific genes such as procyclins, PGKP and others, and one AUUUAUUU motif. The former induces mRNA instability in BF [27, 28] and is recognized by RNA binding protein Rbp10 [29], and the latter was proposed to be bound by Rbp6 [30].

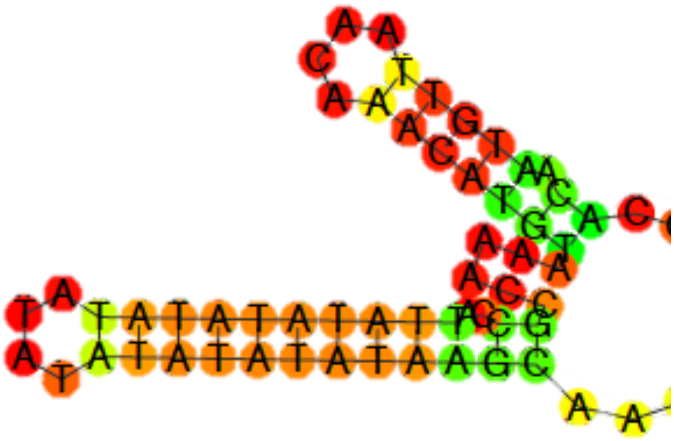

Figure 5: Predicted secondary structure in the 3'UTR of TbIF$_1$. The secondary structure was predicted with RNAfold [25]

1.5. Rbp10

The U(A)U$_6$ motif, bound by Rbp10 [29], is frequently present in developmentally regulated mRNAs. Transcripts containing the motif are expressed in PF, whereas they are generally suppressed in BF [29, 31]. Rbp10, a 306 amino acid long protein with the RNA-recognition motif at the N-terminus, is expressed in BF but was not detected by western blot [31] or by proteomic [32] analysis in PF or in the stumpy form of the parasite. PF *T. brucei* with artificially induced Rbp10 expression differentiated into BF, suggesting that the RNA binding protein can act as a regulatory switch in differentiation [32]. Another indication for a regulatory function is that RNA interference (RNAi) of Rbp10 on BF resulted in growth inhibition [31].

1.6. Rbp6

Another RNA binding protein is the developmentally critical Rbp6, which binds to the AU-rich motif AUUUAUUU [30]. In culture, induced expression of Rbp6 resulted in a differentiation of procyclic cells into next developmental stages found in the tsetse fly, i.e. long and short epimastigotes, and metacyclics, representing the stage competent to infect mammalian host. After induction, the kinetoplast localized at the posterior pole and the mitochondrial architecture changed from multibranched to tubular form, which indicates the important role of Rbp6 in the differentiation cascade from noninfectious to infectious cells [33].

2. Aims of the Thesis

1. To determine the effect of the presence of Rbp10 and Rbp6 binding motifs in the $TbIF_1$ 3'UTR on the expression of reporter genes on mRNA and protein level.

2. To compare translation efficiency of the reporters by determining their association with polysomes.

3. Methods and Materials

3.1. Cell culture

3.1.1. Strains and culture maintenance

All cell lines used in this study are derived from *T. brucei* BF Lister 427 strain. The cell lines (Table 1) are grown in HMI-11 medium supplemented with 10% FBS (Table 4) and geneticin (2.5 μg/ml) at 37°C. The transfected cell lines are selected and maintained in the presence of puromycin (0.1 μg/ml). Cells are maintained in the mid-log phase at a density from $5*10^5$ to $1.6*10^6$ cell/ml.

3.1.2. Cell counting

Cells are diluted 200-times by Hemasol and counted with a Z2 Coulter Counter (Beckman).

3.1.3. Preparation and thawing of cryo-stabilates

After successful transfection or cultivation and testing, cryo-stabilates are prepared to conserve the cell lines for future experiments. 500 µl of a liquid culture at a density of $1\text{-}1.5*10^6$ cell/ml and 500 µl of bloodstream-form freezing solution (Table 5) is pipetted into a cryo-vial under sterile conditions. The mixture is kept on ice for 30-60 min and afterwards stored for 1 week at -80°C. After this procedure, which ensures higher survival rates after thawing, the stabilates are transferred to liquid nitrogen for long-term storage.

Stabilates are thawed at room temperature (RT). The content of the cryo-vial is transferred into an incubation flask with 4 or 9 ml of HMI-11 + 10 % FBS medium and the culture is placed in the 37°C incubator. Cell viability is visually inspected until the next dilution.

3.1.4. Cell harvesting

Cells are harvested at densities ranging from $0.5\text{-}0.8*10^6$ cells/ml by spinning in 250 ml conical tubes at 1300 g for 10 min at 12 °C.

3.2. Preparation of cell lines BF427/pOG202 and BF427/pOG207

Two cell lines BF427/pOG202 and BF427/pOG207, which were missing for the expression analysis (marked with a yellow arrow in figure 10), are created by using plasmids constructed previously.

3.2.1. Used plasmid

All constructs in this study are based on pH1437, obtained from C. Clayton, University of Heidelberg. pHD1437 based constructs contain the following main features:

- T7 polymerase promoter/terminator: the T7 polymerase ensures a high expression level

- Chloramphenicol acetyltransferase coding sequence (CAT CDS): reporter gene
- 3’ UTR variants inserted between *Bam*HI and *Xho*I restriction sites
- sequence for homology recombination into the multiple copy β-tubulin locus (Tb427.01.23(3,5,7,9)0; [34])
- Puromycin resistance gene (PAC) serving as a selection marker

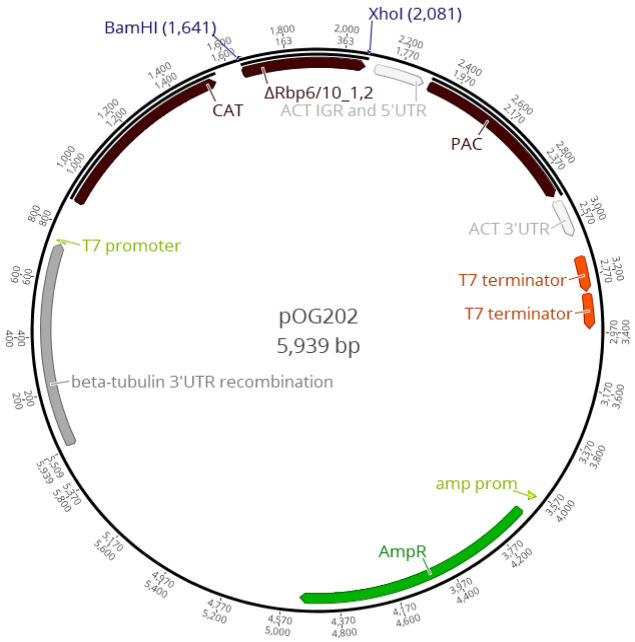

Figure 6: Map of pOG202, which was derived from pHD1437

Table 1 lists all used CAT reporter variants, the respective constructs and its 3’UTR lengths and Figure 6 shows a map of one of the constructs.

Table 1: Plasmids used to create the reporter cell lines; “” indicates plasmids used for cell line creation in the frame of this thesis.*

Plasmid name	**3’ UTR deletions**	**3’ UTR length**
pOG191	none	457
pOG192	Hairpin region (hp)	367
pOG193	Hairpin and U-rich region	266
pOG194	Hairpin, U-rich and Rbp6/10 motif region	191
pOG202*	ΔRbp6/10_1,2	434
pOG203	ΔRbp10_1,2	441
pOG204	ΔRbp10_1	449
pOG205	ΔRbp10_2	449
pOG206	ΔRbp6	450
pOG207*	ΔRbp6/10_1	442

3.2.2. Transfection of BF *T. brucei* using AMAXA instrument and reagents

Plasmid linearization

Digestion is done by *Not*I restrictions enzyme in 100 µl reaction volume (table 7) at 37 °C for 45 min.

Precipitation of linearized plasmid

- Add 10 µl sodium acetate (pH = 5.2) and 250 µl 97% ethanol to facilitate precipitation
- Vortex and incubate in -80 °C overnight (o/n)
- Spin pellet down at 4 °C for 30 min at maximum speed
- Wash with 200 µl 70 % ethanol and vortex
- Spin DNA down at 4 °C for 5 min at maximum speed
- Resuspend pellet in 30 µl sterile water under sterile conditions in TC hood
- Transfer 3 µl to new microtube
- Measure concentration as UV light absorbance at 260 nm by NanoDrop™ using 2 µl
- Add 8 µl water and 1 µl 10x DNA dye added to the 1 µl remaining linearized DNA and run sample on agarose gel to verify the completeness of linearization

Culture preparation

Cultures are brought to an appropriate density to reach density 0.8-0.9*10^6 cells/ml on the day of transfection.

Preparation before harvesting cells for transfection

- Distribute 90 ml HMI-11 medium + 10% FBS in three conical tubes this way:
  30 ml in tube A and 27 ml in tubes B and C
- To prepare AMAXA transfection solution, combine 81.8 µl Human T-cell Nucleofector solution (Table 8, Lonza) and 18.2 µl supplement in a 1.5 ml microtube under sterile conditions
- Add 10 µg of linearized plasmid in cuvette

Done per each transfection

- Harvest 50 ml culture at a density of 0.8-0.9*10^6 cells/ml by centrifugation at 1300 x g for 10 min at RT
- Wash 1x with 20 ml sterile PBS-G (Table 6) and remove all liquid traces
- Resuspend cells in 100 µl transfection solution with the linearized plasmid at 4 °C

- Transfer 100 µl of the mixture to the electro cuvette and place cap on cuvette
- Select preset program X-001 on AMAXA instrument and perform electroporation
- Transfer all content of the cuvette to tube A
- Mix well and transfer 3 ml to tube B
- Mix well and transfer 3 ml to tube C
- Distribute 1 ml aliquots of each dilution step in its own 24 well plate and incubate at 37 °C
- After 16 h: prepare 75 ml of medium containing antibiotic of parental cell line (Geneticin, c = 2.5 µg/ml) and 2x concentration of selection antibiotic (Puromycin, c = 0.1 µg/ml)
- Add 1 ml selection medium to each well

Typically, positively transfected cells are seen after 5 days.

3.2.3. Cell line selection

Transfected cell dilution series in 24 well plates is regularly checked over a period of one week and several clones are chosen for verification.

3.2.4. Cell line verification

Integration of CAT containing cassette selected clones are verified by PCR after genomic DNA (gDNA) extraction (see 3.3.1.). Product lengths vary depending on the 3'UTR length. Figure 7 shows the annealing region for cell line verification primers.

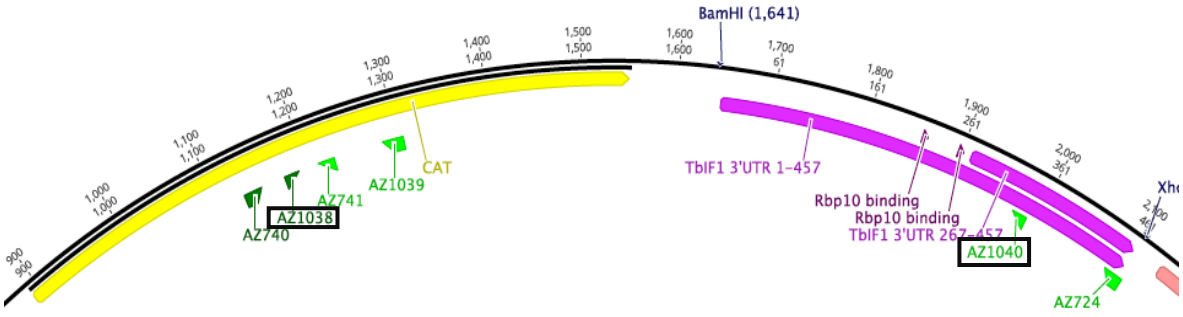

Figure 7: Cell line verification primer annealing region. Yellow: CAT CDS; Purple: 3'UTR variants

AZ1038: CCATGAGCAAACTGAAACG

The forward primer is complementary to CAT CDS.

AZ1040: GTGACCCGAATAGAAAACC

The reverse primer is complementary to part of 3'UTR common to all construct variants.

3.3. RNA and DNA isolation and processing

3.3.1. gDNA extraction

For gDNA extraction, cells are washed with 1 ml PBS-G and stored at -80 °C or resuspended in 1 ml PBS-G and directly processed. gDNA is extracted using the GenElute™ Mammalian Genomic DNA Miniprep Kit (Merck). The described protocol for cell cultures is derived from [35]:

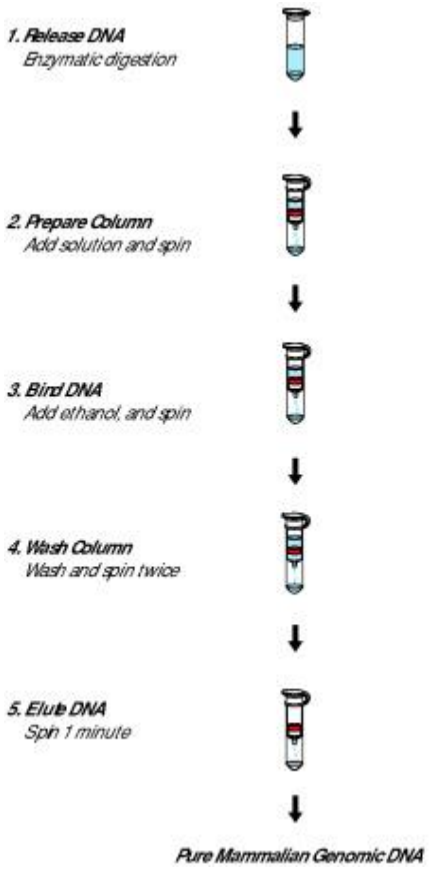

Figure 8: gDNA extraction scheme [36]

- Harvest 100 ml cells at a density of $0.8*10^6$ cells/ml by
- Wash cells with 1 ml PBS-G and spin down
- Resuspend cells in 200 µl resuspension solution
- Add 20 µl RNase A Solution and incubate on RT for 2 min.
- Lyse cells by the addition of 200 µl of Lysis Solution C and add 20 µl proteinase K to degrade proteins
- Vortex sample roughly for 15 seconds and incubate at 70 °C for 10 min
- In the meantime, prepare column by addition of 500 µl Column Preparation Solution and centrifugation at 12000 x g for 1 min
- Add 200 µl of 96% ethanol to the lysate and homogenize by 5-15 seconds vortex
- Transfer total content of the microtube to the treated binding column with a wide-cut pipet tip to minimize DNA shearing
- Perform centrifugation at 7000 x g for 1 min
- Discard the tube with the flow-through and place the binding column in a new 2 ml collection tube
- Wash step 1: add 500 µl Wash Solution, centrifuge at 7000 x g for 1 min.
- Discard tube containing the flow-through and place binding column in a new 2 ml collection tube
- Wash step 2: add 500 µl Wash Solution, followed by centrifugation at 14000 x g for 3 min.

- Additional drying step to remove all remaining ethanol: place binding column in a new 2 ml collection tube and spin for 1 min at 14000 x g
- After discarding the collection tube containing ethanol, place the binding column in a new 2 ml collection tube, add directly 200 µl Elution Solution in the center of the column
- After 5 min incubation on RT, spin column for 1 min at 7000 x g
- gDNA is now in solution in the collection tube

Freeze gDNA at -20 degree for storage or process directly for expression analysis.

3.3.2. Isolation of total RNA

After harvesting 100 ml culture at a density of $0.8*10^6$ cells/ml, the cells for total RNA extraction are washed with 1 ml PBS-G, stored at -80 °C or resuspended in 1 ml PBS-G and directly processed.

- Thaw cells at room temperature (RT) or process directly after harvesting
- Add 1 ml phenol : chloroform : isoamyl alcohol (molar ratios: P:C:I 25:25:1), mix vigorously by vortexing, and spin at 12000 x g at 4 °C for 15 min
- Transfer the upper aqueous phase into new microtube
- Add 1 ml chloroform, mix, and spin at 12000 x g at 4 °C for 15 min
- Transfer aqueous phase into a new microtube
- Add 1 ml isopropanol, incubate 10 min on RT and spin at 12000 x g at 4 °C for 15 min
- Wash pellet with 70 % Ethanol at 12000 x g at 4 °C for 5 min
- Remove supernatant and dry pellet on air for 5 min
- Resuspend pellet in 30 µl RNase-free water and measure RNA concentration on NanoDrop™

3.3.3. DNase treatment

RNA samples supposed for expression analysis are treated with TURBO DNA-free™ Kit (Invitrogen™). The described protocol is derived from [37].

- Up to 15 µg of RNA can be digested in 50 µl reaction volume
- Add 5 µl of 10x buffer and 1 µl DNase
- Add RNase-free water to 49 µl
- Incubate solution at 37 °C for 30 min
- Add 1 µl of DNase

- Incubate solution at 37 °C for 30 min
- Add 5.5 µl of 10x inactivation buffer
- Flick micro tube every 30 seconds while incubation
- Centrifuge samples for 1.5 min at 10000 x g
- Transfer 44 µl of supernatant to fresh microtube

Alternatively, DNase I (RNase-free) from New England Biolabs is used [38]:

- Table 2 shows the reaction composition
- Incubate at 37 °C for 120 min
- Inactivate DNase by phenol/chloroform extraction after volume increase to 1 ml by RNase-free water (analogous to 3.3.2.)

Table 2: DNase I reaction solution

Reagents	**Amount by 100 µl reaction**
RNA	Around 10 µg
DNase I 10x reaction buffer	10 µl
DNase I (RNase-free)	1 µl
RNase-free water	to 100 µl

3.3.4. RNA precipitation and resuspension

- Add 5 µl 3 M sodium acetate pH 5.2, 1 µl RNase-free glycogen and 150 µl Ethanol
- Mix solution well and incubate at -80 °C for 60 min or o/n
- Spin down on maximum speed at 4 °C for 30 min
- Wash with 1 ml 70 % ethanol, spin at maximum speed for 10 min
- Remove supernatant and dry on air for 5-10 min
- Resuspended pellet in 20 µl RNase free water and measure RNA concentration on NanoDrop™

3.3.5. Reverse transcription

Reverse transcription is done using TaqMan™ Reverse Transcription Reagents (Invitrogen™). The described protocol is derived from [39].

- 20 µl reaction efficiently converts up to 400 ng of RNA to cDNA
- Reverse transcription reaction solution see table 9
- Thermocycler conditions see table 3.

Table 3: Reverse transcription thermocycler conditions

Temperature	Time
25 °C	10 min
37 °C	30 min
95 °C	5 min
4 °C	Indefinitely

3.4. $TbIF_1$ expression analysis by reverse transcription qualitative polymerase chain reaction (RT-qPCR)

$TbIF_1$ expression analysis is performed using a 96 well plate, the LightCycler® 480 SYBR Green I Master kit, and the LightCycler® 480 instrument. The described procedure is derived from [40].

3.4.1. Measurement principle

Real-time qualitative polymerase chain reaction is a type of PCR, in which the process of the product amplification is monitored by fluorescence. One of the used dyes is SYBR Green I. The dye intercalates in double-stranded DNA, resulting in a greatly increased fluorescence in comparison to the dye in solution. During the PCR reaction, the increased signal of fluorescence of the SYBR Green I is directly proportional to the amount of amplified double-stranded DNA.

The denatured cDNA is in mixture with a buffer, the primers, and the dye. The background fluorescence of the unbound dye is measured and subtracted in the next measuring cycles. After each amplification cycle the fluorescence signal is measured and so the initial concentration can be calculated. [40]

3.4.2. Sample preparation and experimental setup

- Reference genes: tubulin (TUB) and 18s rRNA
- Prepare a 2 step 10-fold dilution series for all cDNA samples
- Use 10x diluted sample for TUB and CAT measurement and 100x diluted sample for 18s rRNA measurement
- Standards: prepare a 6 step 8-fold dilution series using CAT standard stock (solution of pooled previous cDNA samples from CAT-expressing cell lines)
- Use PCR grade water as non-template control (NTC).
- All samples are measured in triplicates; standards in duplicates

- Concentration of the primer pair: 5 µM of each primer
- Table 10 displays the SYBR Green I reaction composition

Cycling conditions:

Preincubation: 95 °C, 5 min

Amplification:

Number of cycles: 45

Primer annealing time: 10 s

Primer annealing temperature: 60 °C

Extension time: 10 s

Extension temperature: 72 °C

Data evaluation

qPCR data evaluation is performed the following:

Preparative steps with the qPCR software:

- Assign and name replicates
- Calculate standard curve and sample concentrations
- Export sample concentration tables and replicate statistics for further analysis

Analysis by Microsoft Excel:

- Divide mean CAT concentration of triplicates by mean 18s rRNA concentration of respective triplicates
- Normalize CAT expression in all cell lines to the cell line with the full-length $TbIF_1$ 3'UTR (BF/pOG191)
- Plot relative CAT mRNA abundancies to compare the mRNA level of different reporter variants.

3.5. CAT protein determination by ELISA assay

Cell pellets, which were washed in PBS-G and flash-frozen, are used to determine first, the overall protein content by BCA assay using Pierce™ BCA Protein Assay Kit, and second, the CAT content by CAT ELISA kit (Merck). Initially, 50 ml of each culture was harvested.

3.5.1. Measurement principle

The CAT ELISA is based on the sandwich ELISA principle.

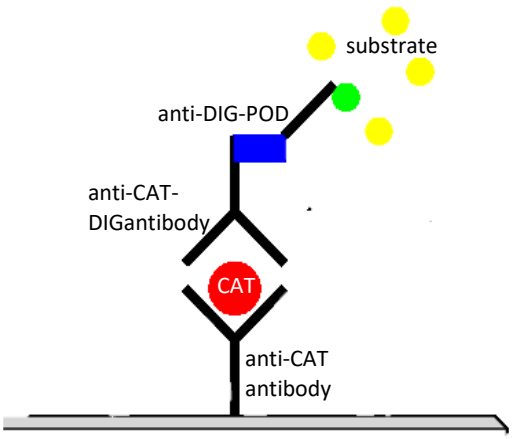

Figure 9: Schematic of the ELISA assay Edited from [41]

Extracts from cells that express CAT enzyme from a reporter construct are added to the wells of a microplate, which is coated with a polyclonal antibody against CAT (anti-CAT). CAT molecules contained in the cell extracts bind to the anti-CAT antibody that is bound to the plate surface. Next, a digoxigenin-conjugated antibody to CAT (anti-CAT-DIG) is added and binds to CAT. In the next step, an antibody to digoxigenin, conjugated to peroxidase (anti-DIG-POD), is added and binds to digoxigenin. In the final step, the peroxidase substrate 2,2'-azino-bis(3-ethylbenzothiazoline-6-sulfonic acid is added. The peroxidase catalyzes the cleavage of the substrate, yielding a colored reaction product. To determine the CAT level, the absorbance at 405 nm and 490 nm is measured photometrically. The absorbance value of the higher wavelength is subtracted from the lower one and the CAT concentration in samples is calculated using a linear regression of subtracted absorbance values of samples with known CAT concentration plotted against the concentration [42].

3.5.2. Total protein determination by BCA assay

The total protein concentration is determined on a 96-well plate using Tecan Infinite M200 plate reader.

The described procedure is derived from [43].

Procedure:

- Concentrations of bovine serum albumin (BSA) standards:
  - 25, 125, 250, 500, 750, 1000, 1500 µg/ml
- Working Reagent (WR) preparation:
  - Mix 50 parts of BCA reagent A with 1 part of BCA reagent B
  - 200 µl WR needed per well
- Lyse flash-frozen cells in 80 µl Lysis buffer (from CAT ELISA kit (Merk))
- Pipette 20 µl of each sample/standard into a microplate well
- Add 200 µl WR to each well and shake plate

- Cover and incubate at 37 °C for 30 min
- Cool down plate to RT and measure absorbance at 562 nm
- Calculate total protein concentration using the standard dilution series:
  The mean blank values are subtracted from the absorbance values at 562 nm. The resulting values are then used to determine the overall protein concentration by inserting them into the absorbance equation. The equation is obtained through generation of the standard absorbance curve by plotting the final absorbance values of the standards (after subtraction of mean blank values) and calculating linear regression. The linear regression equation, in the format of "y = k * x + d ", is then used to calculate the protein concentrations of the samples.
- Dilute samples with the Lysis buffer to a suitable final concentration (based on prior experience and anticipated level of CAT expression) and use these dilutions as 5x sample stocks for CAT protein determination.

3.5.3. CAT protein determination by CAT ELISA

The CAT protein concentration is determined on a 96-well plate. The used machine is Tecan Infinite M200.

The procedure is performed according to the product manual [42].

Data evaluation

Subtraction of absorbance at 490 nm from absorbance values at 405 nm is performed. From this value, the blank absorption value is subtracted. These numbers are then used for the determination of the CAT concentration by inserting them in the absorbance equation. The formula is obtained through generation of the standard absorbance curve by plotting the final absorbance values of the standards and addition of the trendline. The line equation, in the format of "y = k * x + d ", is then used to calculate the different CAT concentrations of the samples.

3.6. Polysome isolation and translation efficiency analysis

750 – 1000 ml culture with a density of $5*10^5$ cells/ml are harvested and directly resuspended in 1 ml PDC buffer (Table 11) or stored in 10 % glycerol (addition of 250 µl of 50 % glycerol stock) at -80 °C. The polysomes are separated by gradient ultracentrifugation and fractions were collected using the Piston Gradient Fractionator™ (Biocomp) equipped with Triax Full Spectrum Flow Cell (Biocomp) and dedicated software (TRIAX software v2.04).

3.6.1. Polysome fractionation protocol

The described procedure is derived from Juan Alfonso and Cristine Clayton protocols, which are revised and optimized by Ondřej Gahura, Sneha Kulkarni, and Sascha Gratzl.

- Lyse harvested cells resuspended in 1 ml of PDC by addition 10 µl of 20 % IGEPAL, followed by incubation on ice for 5 min
- Pass cells through 24 G needle 15 times to facilitate lysis
- Clear lysates by centrifugation at 15000 x g for 10 min at 4 °C
- Important: set aside 100 µl of lysate for total RNA isolation
- While waiting for centrifugation, prepare the sucrose gradient
- Mark SW40 centrifugation tube at the half mark using the marking tool
- Pour 10 % sucrose solution (table 12) until 2-3 mm above the half mark
- Layer 50 % sucrose solution (table 13) under the 10 % solution by the usage of the long needle syringe until the meniscus reaches the half mark
- Give special attention when taking out the needle, do not mix the two layers or release some 50 % sucrose solution in accident
- Place caps on the tubes without forming a bubble inside. Excess solution can remain inside the cap
- Place tube in the gradient maker rack for SW40 and balance by an identical prepared tube
- Place the rack in the center of the pre-leveled gradient station platform
- Use following gradient profile setting: SW40, long, sucrose, 10-50 %
- After gradient preparation, suck up excess sucrose solution with a paper towel and carefully remove the caps
- Load 850 µl of sample supernatant on top of the gradient
- Balance tubes on the digital balance with 10 % sucrose solution and place them in the SW40 buckets
- Close the buckets using the provided tool
- Place the buckets in the rotor and centrifuge at 36000 rpm for 2 h and 4 °C
- While the centrifuge is running, prepare the fraction isolator
- Switch on the gradient station, select SCAN, and start the computer
- Remove storage 20 % ethanol from the syringe
- Rinse station with MiliQ for 10 s
- Open TRIAX software at the computer and select the SW40i rotor

- Run settings:
    - Tube length: 83.8 mm
    - Volume displaced/mm: 0.143 ml/mm
    - Number of fractions: 12
    - Fraction volume: 1 ml
- Calibrate with MiliQ
- Open air-valve and flush system with air for 10 s
- Lubricate piston tip with the provided lubricant and screw it on the piston
- Start fractionation and observe the outlet of the fractionator until the first drop of the first fraction appears
- Mark start of first fraction using the digital button “Frac. Adv.”
- Collect fractions in a 96-deep-well block
- After fractionation is finished, flush fractionator with 20 % ethanol
- Leave ethanol in the system to prevent bacterial growth

3.6.2. RNA processing steps

The chosen fractions were processed as follows:

- Transfer fractions to 2 ml microtube
- Add of 1 ml P:C:I
- Store at - 80 °C
- Perform RNA isolation (according to 3.4.2)
- Perform reverse transcription (according to 3.4.5.)
    - Important: prepare control sample without reverse transcriptase (-RT) but with same cycling conditions

3.6.3. Translation efficiency analysis by RT-qPCR

Translation efficiency analysis is performed using a 96 well plate, the LightCycler® 480 SYBR Green I Master kit and the LightCycler® 480 instrument. For the following protocol, [40] is used as a template and altered to fulfill the needed conditions.

Sample preparation and experimental setup:

- Prepare a 2 step 10-fold dilution series for all fractions
- Use the 10x diluted sample for TUB and CAT measurement and 100x diluted sample for 18s rRNA measurement

- Standards: prepare a 6 step 8x dilution series using CAT standard stock (solution of pooled cDNA samples from CAT expressing cell lines)
- Use PCR grade water as non-template control (NTC).
- Measure all samples in triplicates and standards in duplicates
- Concentration of the primer pair: 5 µM of each primer
- Table 10 displays the SYBR Green I reaction composition

Cycling conditions:

Preincubation: 95 °C, 5 min

Amplification:

Number of cycles: 45

Primer annealing time: 10 s

Primer annealing temperature: 60 °C

Extension time: 10 s

Extension temperature: 72 °C

Data evaluation

qPCR data evaluation is performed the following:

Preparative steps with the qPCR software:

- Assign and name triplicates
- Calculate standard curve and sample concentrations
- Export sample value table and replicates for further analysis

Analysis by Microsoft Excel:

- Divide mean CAT concentration of triplicates by mean 18S rRNA concentration of respective triplicates
- Do the same for the mean TUB concentration
- Normalize the yielded relative CAT mRNA abundancies by the standardized CAT input content
- Plot these values to compare the effect of the 3'UTR on the translational efficiency of different reporter variants.

3.7. Recipes of Solutions and Reagents

The following tables (4 – 13) contain the recipes of used solutions and the reagents. Tables were referred in the respective method sections.

Table 4: Composition of HMI-11 media with 10% FBS without antibiotics

Reagent	**Amount per 10 l**
Invitrogen HMI-11 premix	181.4 g
NaHCO3	30 g
FBS	1 L
Milli Q water	Adjusted to final volume

Table 5: Bloodstream form Freezing Solution

Reagent	**Final concentration**
Glucose	100 mM
NaCl	72 mM
Sodium Citrate	5 mM
BSA	15 mM
Glycerol	12

Table 6: Phosphate buffer saline with glucose (PBS-G)

Phosphate Buffer Saline with Glucose PBS-G	**Final concentration, pH: 7.4**
NaCl	130 mM
$Na_2HPO_4 \cdot 12\ H_2O$	7 mM
NaH_2PO_4 (anhydrous)	3 mM
Glucose	6 mM

Table 7: AMAXA transfection digestion solution

Ingredient	**Volume**
Plasmid	50 µl (c = 500 ng/ml)
MilliQ	35 µl
10x FD buffer	10 µl
NotI	5 µl

Table 8: Nucleofactor solution, pH = 7.3

Reagent	**Final concentration**
Sodium phosphate pH = 7.2	90 mM
Hepes, pH = 7.3	50 mM
KCl	5 mM
$CaCl_2*2H_2O$	0.15 mM
MilliQ	-

pH adjusted to 7.3 with 1 M Na_2HPO_4 and filter sterilized under sterile conditions

Table 9: Reverse transcription reaction solution (Thermo Fisher Scientific, Invitrogen™ TaqMan™ Reverse Transcription Reagents)

Reagents	**Amount per 20 µl reaction**
DEPC-treated water	to 20 µl
10x reaction buffer	2 µl
25 mM $MgCl_2$	1.4 µl
10 mM dNTP (2.5mM each)	4 µl
100 mM DTT	1 µl
RNase inhibitor	1 µl
Reverse Transcriptase	1 µl
50 µM random hexamer	1 µl

Table 10: SYBR Green I reaction composition (Roche, LightCycler® 480 SYBR Green I Master)

Reagents per well	**Volume used**
2x SYBR Green I master	7.5 µl
Primer pair	0.9 µl (c final = 5 µM)
PCR grade water	1.6 µl
Sample/Standard/NTC (in corresponding dilution)	5 µl

Table 11: PDC buffer composition

Reagent	**Final concentration**
Tris-HCl (pH = 7.4)	10 mM
KCl	300 mM
MgCl2	10 mM
Add freshly:	
DTT	1 mM
Cycloheximide	100 µg/ml

Table 12: 10 % sucrose solution in PDC

Reagent	**Final concentration**
Sucrose	10 % (w/w)
Add freshly:	
DTT	1 mM
Cycloheximide	100 µg/ml

Table 13: 50 % sucrose solution in PDC

Reagent	**Final concentration**
Sucrose	50 % (w/w)
Add freshly:	
DTT	1 mM
Cycloheximide	100/ml

4. Results

To get insight in the post-transcriptional regulation of $TbIF_1$, a well-established reporter system based on the chloramphenicol acyltransferase (CAT) gene from *Escherichia coli* was used. To identify regions of the 3'UTR responsible for $TbIF_1$ regulation, the CAT coding sequence was fused to various $TbIF_1$ 3'UTR variants and expressed in BF trypanosomes. The effect of the different 3'UTRs on CAT mRNA and protein level was tested by expression analyses by RT-qPCR and by an ELISA assay, respectively. Translational efficiency of the reporter constructs was determined by polysome isolation and RT-qPCR.

4.1. CAT reporter variants

Figure 10 shows all used CAT reporter variants and the respective constructs to identify the 3'UTR regions responsible for post-transcriptional regulation of $TbIF_1$. The ACT cell line has the actin 3'UTR fused to the reporter gene and is used as control.

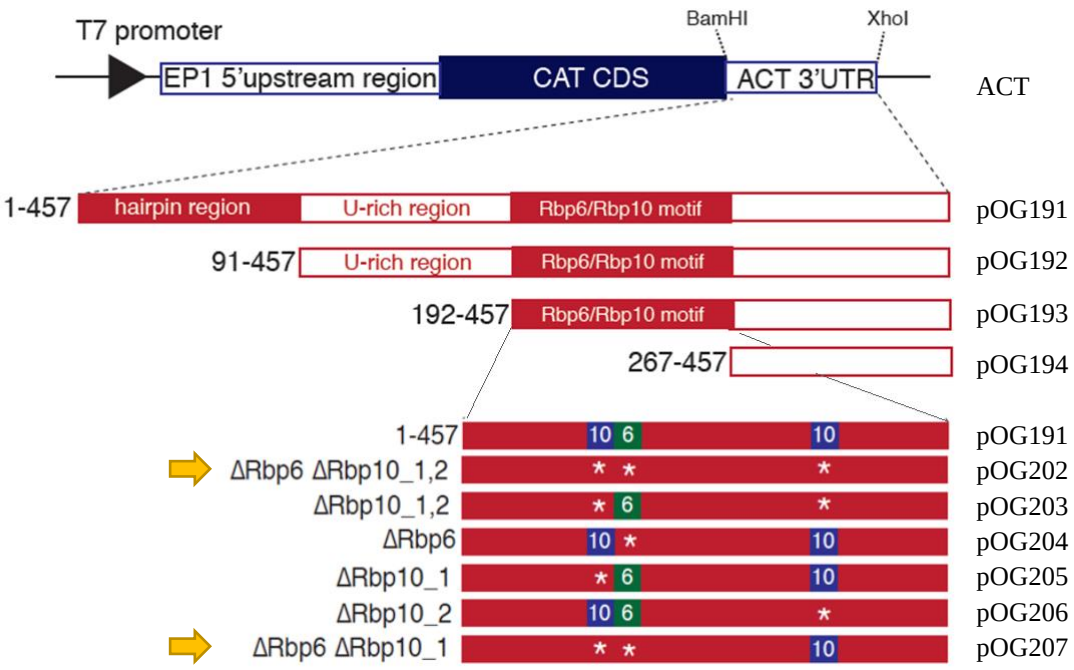

Figure 10: Scheme of CAT reporter variants used in analyses. Deleted binding motifs are marked by "", "10" corresponds to Rbp10 binding motif and "6" to Rbp6 binding motif. Cell lines with reporters marked with a yellow arrow were made in this thesis, all other reporter cell lines were created previously. Plasmid used for cell line creation listed on right side.*

4.2. Preparation of cell lines

In order to create cell lines BF427/pOG202 and BF427/pOG207 expressing the CAT reporters with ΔRbp6/10_1,2 and ΔRbp6/10_1 $TbIF_1$ 3'UTR, parental Lister 427 BF cells

were transfected with plasmids pOG202 and pOG207 linearized by restriction with *Not*I. After the transfection, the antibiotic-resistant clones were selected, their genomic DNA (gDNA) was extracted, and PCR was used to verify the presence of CAT coding sequence (Figures 11 and 12). In total, 6 and 5 clones of BF427/pOG202 and BF427/pOG207 respectively selected and verified. The doubling time for the parental cell line (wild-type, wt) is approximately seven hours, which was also the case for some clones; but a lot of clones were growing at slower rates, with varying doubling times lasting up to more than 12 hours. A possible explanation is that high CAT expression is toxic to trypanosomes and causes growth retardation [44]. Following clones were chosen for further experiments:

BF427/pOG202: A1-A3, B1-2, C1

BF427/pOG207: A1-A5

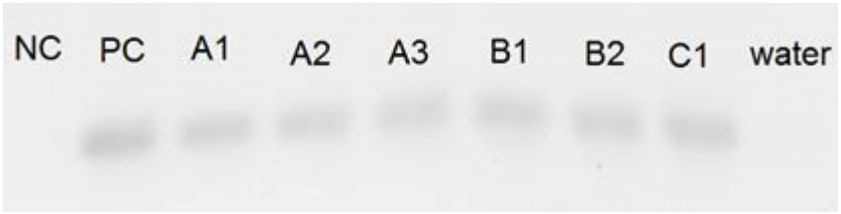

Figure 11: Verification of BF427/pOG202 clones. Ethidium bromide-stained PCR amplification products on the agarose gel after 35 cycles for the positive control (PC) and the BF427/pOG202 clones A1, A2, A3, B1, B2, and C1. For amplification, 11-35 ng of gDNA was used as template. No bands are visible for the negative control (NC), which contains gDNA from the wt procyclic strain PF427 and for the non-DNA control (water), where water was used instead of template DNA.

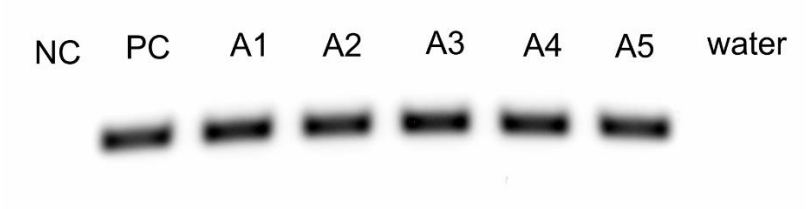

Figure 12: Verification of BF427/pOG207 clones. Ethidium bromide-stained PCR amplification products on the agarose gel after 35 cycles for the positive control (PC) and the BF427/pOG207 clones A1, A2, A3, A4, and A5. For the amplification, 40-70 ng of gDNA was used as template. No bands are visible for the NC, which contains DNA from the wt procyclic strain PF427 and for the non-DNA control (water), where water was used instead of template DNA

4.3. Measurement of relative CAT mRNA levels in reporter strains

The CAT mRNA levels expressed in the reporter strains were determined by RT-qPCR after total RNA isolation and DNase treatment. Figure 13 shows the measured mRNA levels relative to the reporter with the wt $TbIF_1$ 3'UTR (BF427/pOG191, 1-457).

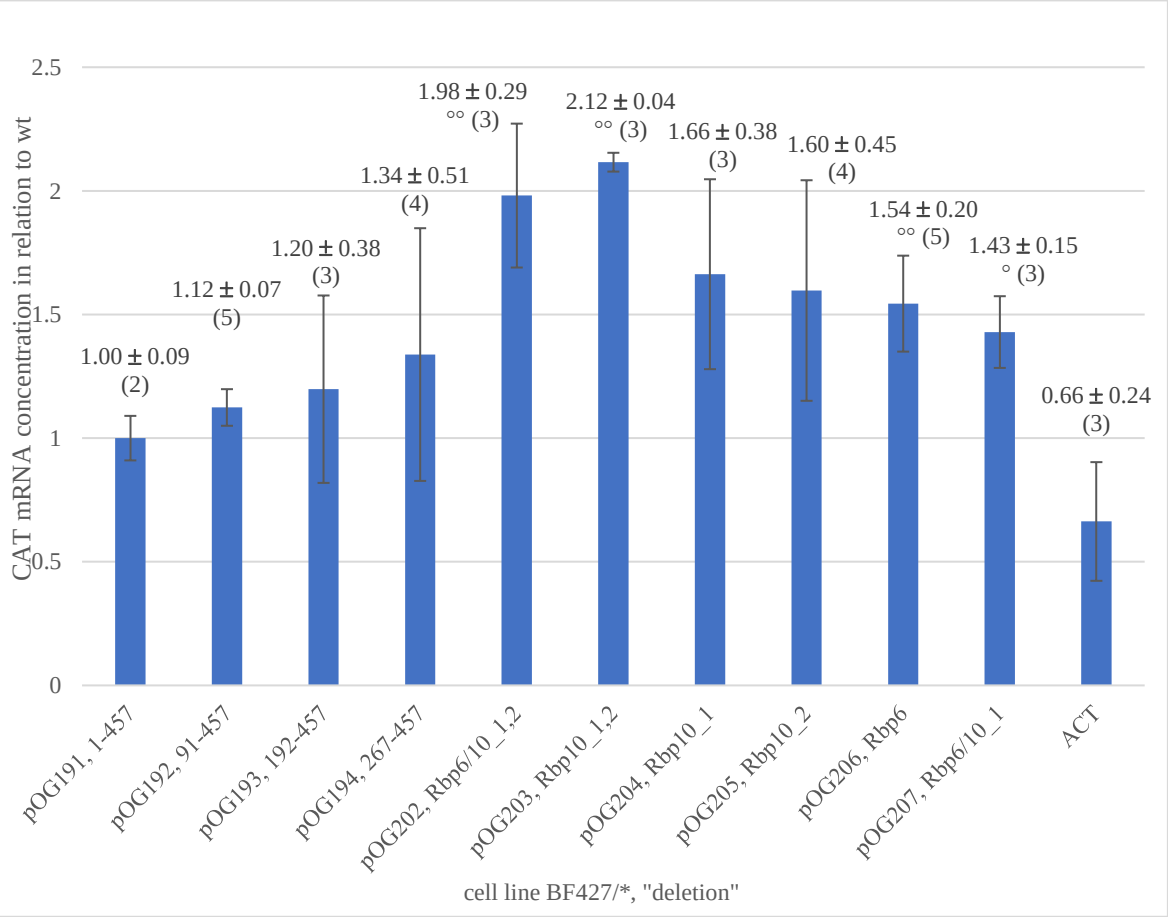

Figure 13: CAT mRNA levels in reporter strains. The values are normalized to the level in the pOG191, 1-457 strain. Error bars indicate SEM. Respective values are depicted above the bars. Number of measurements is shown in parenthesis. Significant differences to BF427/pOG191 are marked with "°°" ($p < 0.05$) or "°" ($p < 0.1$).

The CAT mRNA levels in general are 1.5- to 2-fold elevated in the case of the deletion of the region 1-266 (containing all studied Rbp binding motifs) and single motif deletions, but some differences between are statistically insignificant.

To express the significance of differences of CAT mRNA levels between all reporter combinations, the p-values of the one-sided heteroskedastic T test performed on the CAT mRNA concentrations (table 14). This specific T test is used, because deviation in one direction is assumed and hetero-distributed variances were determined (calculation table in Appendix 2). Significant increase ($p < 0.05$) in comparison to the full length 3'UTR is seen for ΔRbp6/10_1,2, ΔRbp10_1,2 and ΔRbp6.

Table 14: p-values of the one-tailed heteroskedastic (different variance) T test performed on the relative mRNA concentrations. Marked values show significant difference (yellow: p < 0.05; light orange: p < 0.1) between reporter variants.

Cell line BF427/*	**3'UTR variant**	**1-457**	**91-457**	**192-457**	**267-457**	**ΔRbp6/10_1,2**	**ΔRbp10_1,2**	**ΔRbp10_1**	**ΔRbp10_2**	**ΔRbp6**	**ΔRbp6/10_1**
pOG192	91-457	0.190									
pOG193	192-457	0.328	0.432								
pOG194	267-457	0.279	0.353	0.418							
pOG202	ΔRbp6/10_1,2	0.034	0.045	0.091	0.165						
pOG203	ΔRbp10_1,2	0.013	0.000	0.068	0.113	0.344					
pOG204	ΔRbp10_1	0.111	0.147	0.219	0.316	0.274	0.180				
pOG205	ΔRbp10_2	0.138	0.185	0.263	0.358	0.252	0.164	0.457			
pOG206	ΔRbp6	0.026	0.049	0.237	0.363	0.141	0.020	0.400	0.460		
pOG207	ΔRbp6/10_1	0.076	0.118	0.308	0.437	0.098	0.057	0.308	0.371	0.330	
ACT	ACT	0.148	0.093	0.155	0.148	0.013	0.012	0.052	0.066	0.020	0.037

4.4. Comparison of CAT protein expression in reporter cell lines

The CAT protein levels expressed in the reporter strains were determined by ELISA assay and normalized to the total protein concentration determined by BCA assay. Figure 14 shows the relative CAT concentrations in comparison to strain BF427/pOG191.

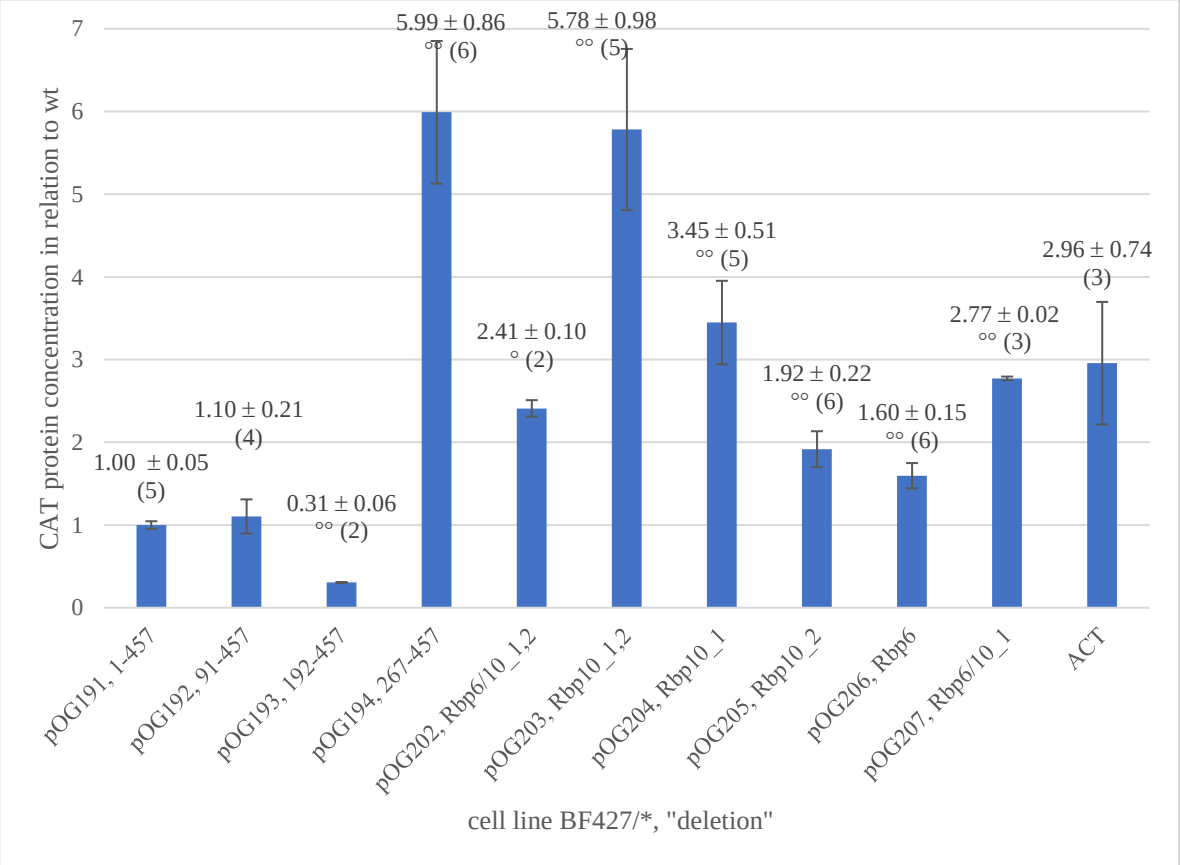

Figure 14: Error bars indicate SEM. Respective values are depicted above the bars. Number of measurements is shown in parenthesis. Significant differences to BF427/pOG191 are marked with "°°" ($p < 0.005$) or "°" ($p < 0.01$)

The deletion of the first 3'UTR region (nt 1-90) or the first and second region (nt 1-191) does not result in an increase in CAT protein level. Thus, we conclude that no important regions, which would suppress translation, are present up to nt 191. The removal of the region 1-266 lead to a high increase in CAT protein level. As all Rbp6 and Rbp10 binding motifs are located between nucleotides 192 and 266, the results suggest that these motifs are responsible for the differential expression of the protein level.

The deletion of the whole region containing all Rbp binding motifs leads to a statistically similar increase as the removal of both Rbp10 binding motifs, indicating that the Rbp10 motifs are crucial for translational suppression of the reporter gene in the blood-stream form *T. brucei*. Increase of the protein level is also seen when single Rbp10 motifs are deleted, but it is not as pronounced as in the case of the double deletion. Only a minor increase in

protein concentration is caused by the deletion of the Rbp6 motif, indicating that it is less important for translational control.

To express significance of differences of CAT protein levels between all reporter combinations, the one-sided heteroskedastic T test performed on the CAT protein concentrations was performed (table 15). This specific T test is used, because deviation in one direction is assumed and hetero-distributed variances were determined (calculation table in Appendix 3).

Table 15: p-values of the one-tailed heteroskedastic (different variance) T test performed on the relative protein concentrations. Highlighted values show significant difference (yellow: p < 0.005; light orange: p < 0.01; light green: p < 0.05) between reporter variants.

Cell line BF427/*	**3'UTR variant**	**1-457**	**91-457**	**192-457**	**267-457**	**ΔRbp6/10_1,2**	**ΔRbp10_1,2**	**ΔRbp10_1**	**ΔRbp10_2**	**ΔRbp6**	**ΔRbp6/10_1**
pOG192	91-457	0.330									
pOG193	192-457	0.000	0.015								
pOG194	267-457	0.001	0.001	0.000							
pOG202	ΔRbp6/10_1,2	0.009	0.003	0.015	0.003						
pOG203	ΔRbp10_1,2	0.002	0.002	0.001	0.438	0.009					
pOG204	ΔRbp10_1	0.002	0.002	0.001	0.015	0.048	0.034				
pOG205	ΔRbp10_2	0.003	0.013	0.000	0.001	0.039	0.005	0.014			
pOG206	ΔRbp6	0.004	0.051	0.000	0.001	0.002	0.004	0.006	0.126		
pOG207	ΔRbp6/10_1	0.000	0.002	0.000	0.005	0.079	0.014	0.119	0.004	0.000	
ACT	ACT	0.059	0.060	0.035	0.016	0.269	0.028	0.307	0.147	0.102	0.414

4.5. Translation efficiency determination in association with different 3'UTRs

Lysates of cell line clones BF427/pOG191 A3, BF427/pOG194 B1, BF427/pOG203 B4, and BF427/ACT A5 were ultracentrifuged on a 10-50 % sucrose gradient, monosomal and polysomal peaks were assigned and RNA of corresponding fractions was isolated and reverse transcribed. CAT reporter RNA concentration was determined by RT-qPCR. BF427/pOG191 was taken as full-length 3'UTR reporter, BF427/pOG194 was chosen to see the translational efficiency when the whole region containing all Rbp motifs is deleted, cell line BF427/pOG203 was selected to investigate the contribution of the Rbp10 binding motifs and BF427/ACT served as a control construct with 3'UTR of a housekeeping gene. The above stated clones were chosen because of their viability and availability.

4.5.1. Separation and measurement principle

Actively translated mRNA molecules have a higher number of ribosomes associated with them. Therefore, it is possible to determine the relative translation efficiency if you separate mRNA molecules associated with multiple ribosomes, called polysomes, from the mRNA pool and mRNA, which is only occupied by one ribosome. This monosomal mRNA corresponds to untranslated, or not efficiently translated RNA material. To separate the monosomes from the polysomes, a differential ultracentrifugation of the cell lysates is performed on a sucrose gradient. Because the mRNA-ribosome assemblies have a higher density than the sucrose solution, they travel in the gradient. mRNA with polysomes travel faster because of their higher mass, and so they are found in lower fractions. mRNA from the fractions containing the polysomes is isolated, reverse transcribed and presence of specific transcripts is analyzed by RT-qPCR to determine their abundancies, which is normalized to the total ribosomal content and so the connection between different transcripts and translation efficiency can be drawn.

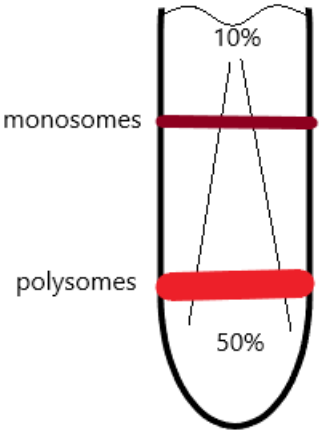

Figure 15: Scheme of a sucrose gradient ranging from 10-50 % with marked regions where monosomes and polysomes can be found approximately

4.5.2. Sucrose gradient fractionation

The sucrose gradients were fractionated and the RNA content in fractions was continuously recorded as absorbance at 260 nm. In the resulted gradient spectrum, the absorption correlates with the concentration of RNA, which allows the identification of the RNA-rich ribosomal fractions. The fraction(s) corresponding to the monosomal and polysomal peaks were chosen for RNA isolation, reverse transcription and RT-qPCR analysis. In addition, for each analyzed cell line, a sample of lysate loaded on the sucrose gradient ('input sample') was processed in the same way as the chosen fractions. Choosing correct fractions for further analysis is crucial, especially assigning the monosomal peak without cutting the peak shoulder on the left side of the monosome peak, as the peak shoulder corresponds to the small ribosomal subunit associated with mRNA and not a full ribosome-RNA assembly. Including it into the monosomal fraction would bias the result calculation, because the 18s

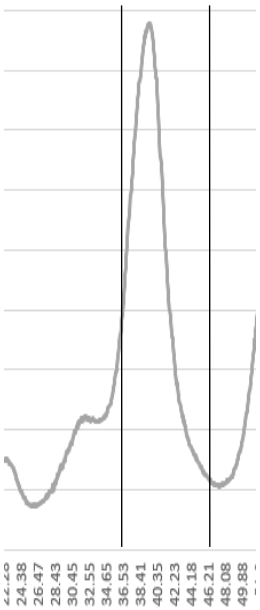

Figure 16: Assignment of the fraction without taking subunit RNA

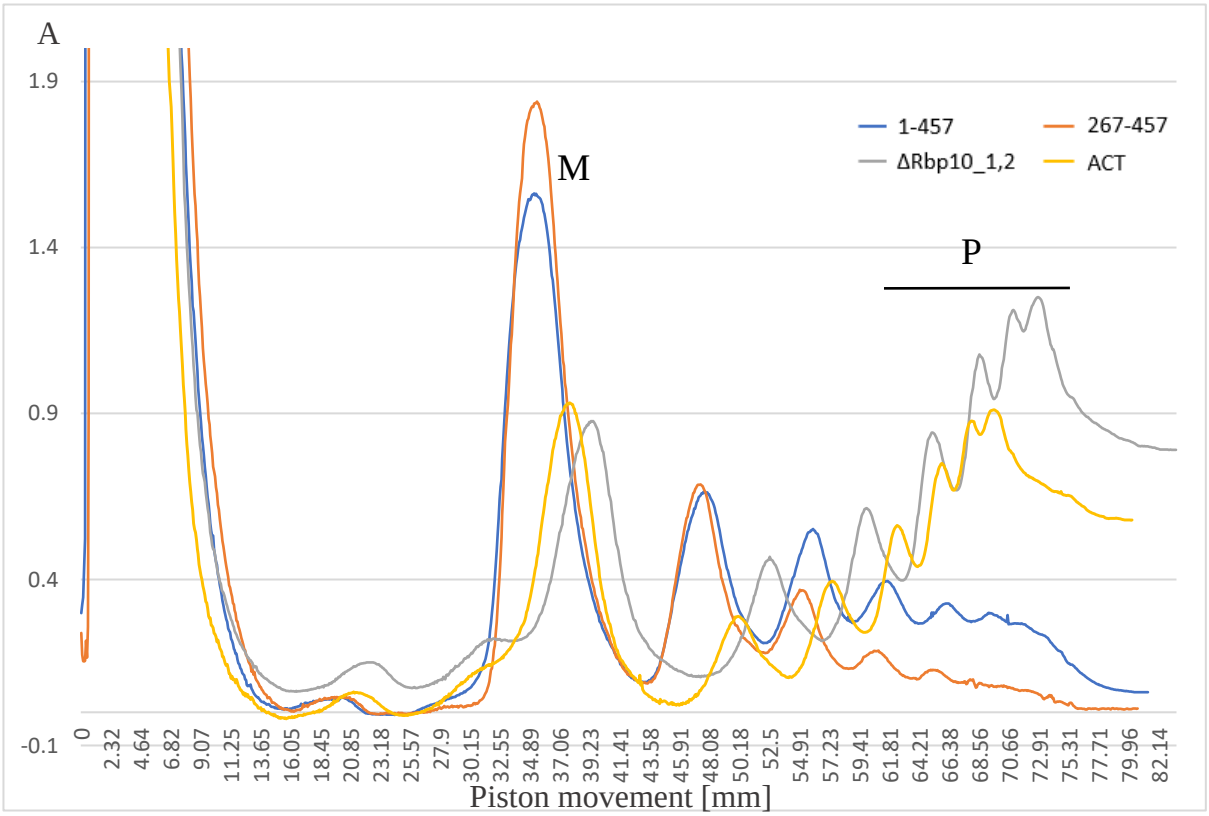

Figure 17: Absorbance profile of translation efficiency determination of reporter construct with following 3'UTR variants: TbIF$_1$ 1-457, TbIF$_1$ 267-57, TbIF$_1$ ΔRbp10-1,2 and ACT. M: monosomal peak, P: polysomal peaks

rRNA is used to characterize the ribosome content and so additional 18s subunit RNA would lead to an overestimation of the monosomal concentration.

4.5.3. Determination of relative CAT and TUB mRNA concentration in individual fractions

The values of CAT mRNA and TUB levels in the respective fractions determined by RT-qPCR were divided by the respective 18s rRNA concentration to normalize to the content of ribosomes (table 16 and 17). The measurement of the TUB association with polysomes serves as control, because the translational state of the TUB gene should not be affected by gene manipulation. Overall, this is in agreement with the resulting numbers (Table 17), taking biological variability and the potential toxic effect of high CAT reporter expression (on RNA or protein level) [44 and see Discussion] into account.

Table 16: CAT mRNA concentration normalized to the 18s rRNA concentration

fraction	1-457	267-457	ΔRbp10_1,2	ACT
input	0.40	1.11	3.20	0.24
M	0.07	0.61	0.79	0.05
P	0.10	1.42	5.90	0.41

Table 17: TUB mRNA concentration normalized to the 18s rRNA concentration

fraction	1-457	267-457	ΔRbp10_1,2	ACT
input	23.87	37.68	41.60	36.71
M	6.56	10.67	7.74	4.18
P	9.62	36.86	30.68	8.10

4.5.4. CAT/18s ratio normalized to input CAT concentration

The CAT concentrations are normalized in the second step to the input CAT mRNA concentration. The reason for this is, that the CAT expression varies significantly between the cell lines. Without the normalization to the CAT input content, a high CAT signal associated with polysomes could reflect high CAT expression rather than high efficiency of translation. The normalized values are given in Table 18.

Table 18: CAT/18s ratio normalized to the input CAT mRNA concentration

fraction	1-457	267-457	ΔRbp10_1,2	ACT
input	1	1	1	1
M	0.18	0.55	0.25	0.23
P	0.27	1.28	1.84	1.72

The values normalized to the results of the reporter 1-457 can be seen in Table 19.

Table 19: Values of fractions of table 8 compared to 1-457 clone A3

fraction	1-457	267-457	ΔRbp10_1,2	ACT
M	1	3.09	1.40	1.27
P	1	4.82	6.95	6.50

We observed a large increase in CAT mRNA (Table 19) associated with polysomes in case of the deletion of the full 3'UTR harboring all Rbp binding sites and in the deletion of both Rbp10 binding motifs in comparison to the wild type 3'UTR variant. We conclude that translational suppression is lost because in both cases the Rbp10 motifs are missing.

5. Discussion

5.1. Experimental discussion

To investigate the contribution of protein binding motifs in 3'UTR of inhibitory factor 1 of the F_1F_0-ATPase in *T. brucei* ($TbIF_1$) on its expression on mRNA and protein level and on translation efficiency, a CAT reporter system was generated. Employment of a CAT reporter series harbors several advantages. It is a widely accepted standard in literature [45] including numerous studies on *T. brucei* [29, 46, 12, 28, 47]. It allows the detection of proteins in two ways – with specific antibodies using ELISA assay or by measuring the activity of the CAT enzyme with radioactively labeled substrates [48]. The detection of enzymatic activity using radioactively labeled substrates was not used to avoid handling of radioactive compounds and because the scintillation counter was not available. We measured the CAT protein levels by ELISA. It was previously used to determine the effect of the 3'UTR elements on gene expression in *T. brucei* [26]. The measurement by ELISA is precise, because it detects protein directly, without an amplification effect of the enzyme activity [49], and it allows cheap and accessible spectroscopic detection [45]. A disadvantage of the CAT reporter system is, that high expression of CAT can be toxic for *T. brucei* and can thus lead to growth inhibition [44]. The CAT system enables to study the impact of 3'UTRs uncoupled from the cognate coding sequence. On one hand the role of the given isolated 3'UTRs sequence can be directly investigated, but on the other hand, the context of the rest of the gene of interest is lost and therefore possible 3'UTR-gene interactions in the case of more complex regulation are overlooked.

The 3'UTR of $TbIF_1$ contains three binding motifs, one for Rbp6 and two for Rbp10. Not all possible combinations of binding motif deletions were used in the CAT reporter series. Due to time and cost-efficient reasons, only the most relevant combinations, for example the triple deletion of all motifs, the deletion of just the Rbp6 motif, or the presence of only the Rbp6 motif and multiple variants of Rbp10 combinations were assayed.

The cell line verification (incorporation of CAT construct into the genome) was done by PCR using two primers in the coding sequence of the CAT enzyme, which lead to falsely positive results in negative controls (Fig. 18). The gene for the CAT used as the reporter comes originally from *E. coli* [50]. As this organism is widely used in the laboratory, there is a high contamination risk of PCR reactions by this bacterium or its DNA, which we experienced. Therefore, we chose one primer to anneal to the CAT coding sequence and constructed a second primer complementary to a part of the 3'UTR region common to all reporter variants. This combination ensured specificity to positively transfected cell lines

because no other strains in the laboratory, or other possible contaminants, have this combination in the genome. Therefore, no falsely positive results were obtained and so the verifications were reliable.

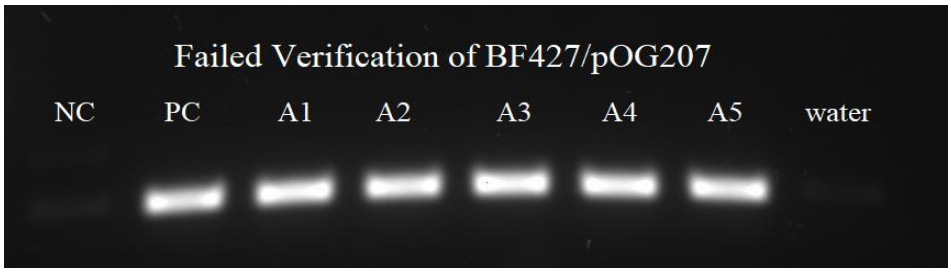

Figure 18: Unsuccessful verification of BF427/pOG207 using two primers annealing to CAT CDS. Amplification bands are seen in the negative control (cell line without CAT reporter) and the water control

The analysis of the samples from polysome fractionation with RT-qPCR represents a novel approach to determine the translational state of a selected gene or reporter gene fused to different 3'UTRs [29]. In the frame of this thesis, the protocols provided by Juan Alfonso and Cristine Clayton labs were revised and optimized and a working protocol was established after multiple runs of troubleshooting and error analysis. Optimization resulted in the following findings: cell pellets for polysome fractionation cannot be washed after harvesting with PBS-G to remove traces of media, in contrast to samples for mRNA expression analysis, because prolonged sample manipulation might lead to dissociation of ribosomes from mRNA. The pellets were directly resuspended in buffer containing cycloheximide, which inhibits translational elongation [51], to maintain polysomes intact. For the same reason the sucrose solutions must be prepared with cycloheximide. The samples must be fractionated immediately after the ultracentrifugation to obtain sharp peaks and prevent diffusion and it is needed to take special care when lubricating, cleaning, and changing the piston tip. The lubricant must not be applied on the inside of the tip but on the whole circumference as a medium thick film. As the sucrose solution leaves a sticky and interfering surface after evaporation, it is crucial to change the tip after each run, to clean it with MilliQ and to re-lubricate it accurately. Perfect perpendicular piston movement into the tube is not essential, but the correct handling of the piston tip is critical. A test run with distilled water before the first fractionation should be done in any case, because the software can fail leading to the loss of the sample. These problems should be diagnosed and solved in the frame of a test run. The RT-qPCR data analysis requires two normalization steps. First, the mean CAT concentration of the fractions is divided by mean 18S rRNA concentration of the respective fractions to normalize the CAT mRNA content to the ribosome content. The same calculation is done for the mean TUB

concentration to show that the genome alterations do not affect the general translation. In theory, the normalized TUB values should be the same in the corresponding fractions in all strains (e.g. all monosomal ratios should be equal). Finally, the calculated CAT/rRNA ratios of the fractions are divided by the normalized CAT content of the input, to standardize to the different CAT expressions in individual reporter cell lines. The second step could be omitted if the expression between the reporters would be the same, which is not the case.

5.2. Result discussion

Measurement of CAT mRNA abundancies revealed that the presence of Rbp10 binding motifs had a mild effect on mRNA destabilization. The mRNA level of the reporters increased 1.5 - 2 times compared to the full-length 3'UTR when the Rbp6/Rbp10 motif region (nt 192-266) was altered by motif deletions. The mRNA level is significantly increased in the case of ΔRbp6/10_1,2, ΔRbp10_1,2 and ΔRbp6 reporter variants in comparison to the full-length and the 91-457 variant (Fig. 13), but the increase was higher in both cases with the double Rbp10 binding motif deletions than in the case of single Rbp6 binding motif deletion. A similar increase was expected for the 267-457 variant, which lacks all Rbp binding motifs, but the measured increase was not significant. The CAT mRNA abundance for this construct exhibits high variability between clones. The high variability can be caused by the fact that a large part of the 3'UTR is missing or because of mistargeting when incorporated into the genome. The exact recombination site was not verified and therefore basal level of transcription in clones can differ, possibly affecting mRNA level. There is a significant difference in the ΔRbp10_1,2 in comparison to ΔRbp6 indicating that the Rbp10 motif deletions are responsible for the increase. The increase of the mRNA level in the case of the Rbp6 deletion can be explained by the proximity of the Rbp6 binding motif with one of the Rbp10 binding motifs (there are no nucleotides between the two binding motifs. see Appendix 1). Rbp6 binding might enhance the binding of Rbp10 and the absence of Rbp6 motif can thus indirectly contribute to the increase of the reporter expression. The highest increase is caused by the double deletion of the Rbp10 motifs (Figure 13) and therefore we conclude that the deletion of two Rbp10 motifs is most probably responsible for mRNA stabilization. Nevertheless, the observed rather mild mRNA increase does not correspond to the increase in protein level or translation efficiency.

On the protein level, a significant increase was seen after the deletion of the region containing all Rbp binding motifs, indicating that those motifs are important for translational regulation. The same increase was observed after the deletion of both Rbp10 binding motifs.

Both single Rbp10 motif deletions lead to a less pronounced increase in protein level, and therefore we conclude that both motifs are required to completely suppress translation in BF. The minor increase due to the deletion of Rbp6 binding motif can be related to the spatial proximity to the Rbp10_2 motif, which could interfere with the binding of Rbp10, although we cannot rule out that binding of Rbp6 itself directly affects the read-out on the protein level.

Taken together, the slight increase in mRNA level does not explain the much higher increase in the protein level. It appears that Rbp10 reduces to some extent mRNA stability but has a much more pronounced effect on protein translation. Similar behavior was seen for the COXV-3'UTR; deletion of its part containing the Rbp10 binding motif had only a weak effect on mRNA level, but the protein level increased significantly [28]. Comparable results were obtained when investigating the influence of a different Rbp in the differentiation of *T. cruzi* [52]. The data of the translation efficiency determination supports this argument (see below). We conclude that binding of Rbp10, but not of Rbp6, is responsible for translational suppression of $TbIF_1$. The deletion of both Rbp10 motifs increased the CAT reporter concentration similarly as the deletion of the whole region containing all binding motifs. In contrast to this, the Rbp6 motif deletion only leads to a minor increase in protein level, plausibly explained by interference with the second Rbp10 binding motif.

Translation efficiency analysis by polysomal fractionation in combination with RT-qPCR revealed, that a significant increase in CAT mRNA (table 19) associated with polysomes could be detected in case of the deletion of the full 3'UTR region harboring all Rbp binding sites and in the deletion of both Rbp10 binding motifs in comparison to the full-length 3'UTR variant. Both variants without the Rbp10 binding motifs exhibited similar efficiency of translation as a control reporter with a 3'UTR of the house-keeping gene actin, which is supposedly efficiently translated in the exponential growth phase, in which the cells were when harvested. We conclude that translational suppression is lost because in both deletion variants tested the Rbp10 binding motifs are missing. This finding is in agreement with the data from the ELISA experiment and together document that the Rbp10 binding motifs are responsible for the translation inhibition of $TbIF_1$ in bloodstream-form *T. brucei*.

5.3. Other factors which can influence $TbIF_1$ expression on RNA and protein level

There are other factors that could affect the $TbIF_1$ expression on mRNA level, but some possibilities were already excluded by experiments in the frame of this thesis or previous investigations (unpublished, Ondřej Gahura). In this thesis, we ruled out an effect of the AU-rich sequence, which is involved in the regulation of procyclic-specific genes [24], or of an alternative splicing binding motif of hnRNP F/H (AAGAA) [53]. Both of these motifs are located in the part of $TbIF_1$ 3'UTR, whose deletions did not affect the reporter expression. Hypothetically, regulation can be mediated also by the 5'UTR [54], which we did not include in the analyses. However, in general, trypanosomal regulatory elements are localized in the 3'UTR [9]. Therefore, a possibility, that $TbIF_1$ expression is regulated via the 5'UTR (or a regulatory element in the coding sequence) is rather low.

Another factor that could influence $TbIF_1$ expression are other RNA-binding proteins, which could either fine-tune the activity of Rbp10 or bind other sequence motifs, and thus affect mRNA stability or translation of $TbIF_1$ in BF. In this thesis, only the contribution of the Rbp10 and Rbp6 motifs, not the bound protein itself was investigated. A further possibility is that Rbp10 and Rbp6 act cooperatively.

Additional regulation on protein level cannot be ruled out because the CAT reporter system does not allow to directly investigate the stability and turnover of $TbIF_1$ protein. $TbIF_1$ could be directed to degradation in BF or chaperones recruitment could increase its stability in PF.

The level of transcription of the CAT reporters, and therefore also outcome of our experiments, depends on the specific location in the genome. The reporter cassette is targeted to the tubulin locus with multiple copies of alpha and beta tubulin genes. The exact position in the locus should not affect the expression, because the locus is transcribed within a single operon [55]. However, we have not verified the site of incorporation and therefore, we cannot exclude that a complete mistargeting of the construct into another part of the genome might have affected the expression in some clones.

5.4. Comparison of reporter mRNA measurements with previously performed $TbIF_1$ expression measurements

Several other studies [21, 22, 29, 46, 53, 54, 56-59; see table 20], detected mRNA of $TbIF_1$ in their high throughput RNA-seq experiments. The experiments either compared transcriptomes of BF and PF or determined impact of various regulatory factors, which are

involved in gene expression regulation, including an alternative splicing-factor, a zinc finger protein, or an RNA helicase, on transcriptome-wide level. In general, multiple studies independently supported differential expression of $TbIF_1$ in PF and BF that we observed on single-gene level (Figure 3).

Table 20: $TbIF_1$ differential expression in other studies

Study	**Specification**	**mRNA**
Butter et al., 2012 [56]	Ratio BF/PF,	0.31 (protein BF/PF ratio: 0.029)
Vasquez et al., 2014 [22]	Ratio BF/PF	0.26
Mulindwa et al., 2015 [57]	Ratio BF/PF	0.15
Mugo et al., 2017 [29]	Ratio BF/PF	0.27
Mugo et al., 2017 [29]	polysomal associated mRNA ratio BF/PF	0.20
Vasquez et al., 2014 [22]	ratio of ribosome-bound/general mRNA level in PF	3.67 (PF) 1.73 (BF)
Erben et al., 2014 [58]	genome-wide screen to find post-transcriptional regulating proteins	Not detected in BF
Kumar et al., 2013 [53]	hnRNAP F/H homologue RNAi	BF: 2.7x upregulated
Singh et al., 2014 [54]	zinc finger protein ZC3H11 RNAi	BF: 2.13x upregulated PF: 1.71x upregulated
Droll et al., 2013 [46]	1 h heat shock	PF: 9.4x upregulated
Kramer et al., 2010 [59]	Induced helicase DHH1 (wt and E182Q mutant with inactivated ATPase activity)	PF: 1.44x upregulated (wt), 2.25x upregulated (E182Q)

Study	Specification	mRNA
Panicucci et al., 2017 [21]	$TbIF_1$ protein detection by western blot	No protein in BF detected (mRNA not investigated)
Mulindwa et al., 2015 [57]	Short stumpy BF	9.05 – 11.1x upregulated in comparison to cultured long slender BF

The results obtained in the frame of this thesis are in agreement with a previously published study, which aimed to identify mRNAs regulated by Rbp10 and shed light on mechanisms of Rbp10 mediated regulation [29]. It showed that the mRNA of $TbIF_1$ is bound by Rbp10 by co-immunoprecipitation and RNA-seq quantification of Rbp10-bound mRNAs. The elute/unbound ratio of 4.9 ranks the $TbIF_1$ transcript in the middle of the list of all 260 Rbp10-bound mRNAs. Further, the study showed that the $TbIF_1$ mRNA level is higher in PF than in BF, which is in agreement with other high-throughput studies (table 20) as well as with our previous results (Figure 3) and it was documented by analyses of mRNAs associated with polysomes, that the translational efficiency of $TbIF_1$ is significantly higher in PF than in BF (polysomal associated mRNA ratio PF/BF 5.06). The study revealed no significant change of $TbIF_1$ mRNA levels in BF after Rbp10 downregulation by RNAi nor in PF after artificial induction of Rbp10. The minor increase in CAT reporter mRNA abundancy caused by the Rbp10 motif deletion, which we observed in this study, is in perfect agreement with the absence of $TbIF_1$ mRNA change upon Rbp10 RNAi in BF cells. The data from [29] in combination with the results from this thesis, namely the mRNA and protein concentration determinations and the detected pronounced effect on translation efficiency, indicate that the major part of the life stage specific $TbIF_1$ regulation is mediated by Rbp10 and occurs on translation level.

5.5. Comparison of polysomal fractionation results with known ribosome profile datasets

Ribosome profiling [22] suggested that the translational efficiency of $TbIF_1$ mRNA is higher in PF (ratio of monosome footprint/general mRNA level: 3.67) than in BF (1.73), which agrees with the stage specificity of the protein [21].

Polysome fractionation is a precise technique that can be adapted to various organisms [60]. It is well established and widely used to investigate differential translation in eukaryotes [61]. The technique is widely used in combination with high-throughput sequencing [62, 63], including in trypanosoma [64], but in it has not been used to study translational regulation mechanism of a single gene in trypanosomes.

The ribosomal absorbance profiles we observed (Figure 17) appear in two different shapes. While one shape shows increasing intensity in heavier polysomes, the other curve is flattening out. The profile in [22] is similar to the flattening curves in figure 17, in contrast to the recorded profiles in [29] or [60], which follow the pattern of increasing intensity at higher polysomes as seen in figure 17. In [60] and [65] intermediate profile shapes are found as well. We reason that a direct comparison of the samples showing different ribosomal profiles is valid as various profiles appear in published ribosome profiles from trypanosoma and other organisms (Figure 19). On the other hand, seeking advice from an expert in the ribosome profiling, we discussed our data with Nicholas Ingolia (UC Berkeley). In his opinion, the polysome profiles should be consistent between the cell lines. He pointed out that even minor irregularities in the growth phase when harvesting the cells, the timing of cycloheximide treatment or random nuclease contaminations can

A:

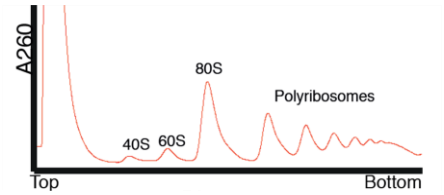

B:

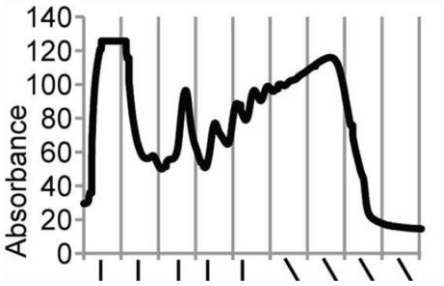

C:

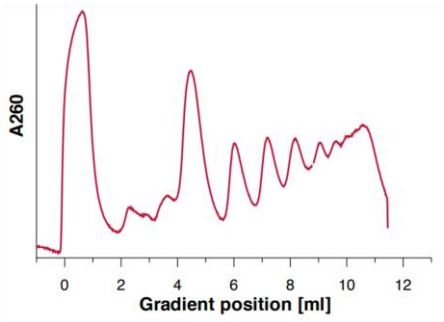

D:

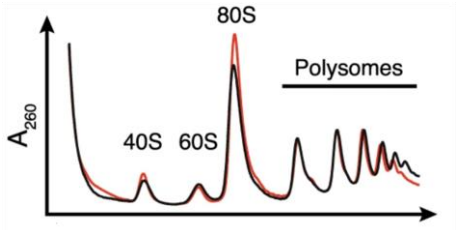

Figure 19: Different ribosome profile shapes in literature. A: T. brucei BF [22]. B: T. brucei BF [29]. C: Saccharomyces cerevisiae [60]. D: Saccharomyces cerevisiae [65]

influence the loss of heavy polysomes. Therefore, the experiments will be repeated to ensure consistency between the profiles and reproducibility of results.

5.6. Additional proposed experiments

An analogous set of experiments with CAT reporters can be performed in PF cells. Because Rbp10 is not expressed in PF, it is expected that the Rbp10 motif deletion would have no influence. Our preliminary data are in agreement with this hypothesis.

Further experiments include the mRNA level monitoring of CAT reports after the inducible differentiation of PF to pre-infectious metacyclic form. The Zíková laboratory established a procedure to induce differentiation of PF to metacyclics by overexpression of Rbp6 (unpublished). One of the genes induced during the differentiation is Rbp10. The expression of Rbp10 itself in PF can induce a metacyclic-like phenotype [29]. Therefore, analyses of expression of our CAT reporters after Rbp6 (or Rbp10) induction could provide additional insight into the regulation of $TbIF_1$.

A direct interaction of Rbp10 to $TbIF_1$ mRNA and CAT reporter transcripts with or without Rbp10 binding motifs can be tested by co-immunoprecipitation (coIP) of Rbp10-bound mRNAs and subsequent detection of $TbIF_1$ mRNAs by RT-PCR. Previously, a similar Rbp10-coIP experiment followed by RNA-seq analysis of bound transcripts suggested association of Rbp10 with $TbIF_1$ mRNA [29]. We attempted to reproduce the experiment and detect endogenous $TbIF_1$ mRNA with RT-PCR using gene-specific primers in the Rbp10-bound pool of mRNAs, but the initial trial was inconclusive, and we could not repeat it due to the lack of anti-Rbp10 antibody.

An alternative approach would be the direct identification of proteins interacting with $TbIF_1$ mRNA or a derived reporter molecule, which could capture additional players in $TbIF_1$ regulation. However, RNA-centric techniques for the identification of RNA-protein interactions are technically demanding and not well established [66]. The expected hypothetical interaction is most likely dynamic and transient, decreasing the chance of success of this type of experiment.

6. Conclusions

- The effect of $TbIF_1$ 3'UTR modification on the expression of CAT reporters on RNA level is rather insignificant.
- The removal of Rbp10 binding motif(s) from $TbIF_1$ 3'UTR results in a 4 to 6-fold increase of the CAT reporter protein level.
- The deletion of the Rbp6 binding motif has no major impact on the CAT protein level.
- The removal of the Rbp10 binding motif leads to an increased association of the CAT-$TbIF_1$-3'UTR mRNA with polysomes, documenting increased translation efficiency when Rbp10 binding is abolished.

We conclude that Rbp10-binding motifs are responsible for negative regulation of $TbIF_1$ expression in the BF form of *T. brucei* and that the regulation occurs predominantly by suppression of translation.

7. References

[1] Franco, J. R., Simarro, P. P., Diarra, A., & Jannin, J. G. (2014). Epidemiology of human African trypanosomiasis. Clinical epidemiology, 6, 257–275. https://doi.org/10.2147/CLEP.S39728

[2] Morrison, L.J., Vezza, L., Rowan, T., Hope, J.C. (2016). Animal African Trypanosomiasis: Time to Increase Focus on Clinically Relevant Parasite and Host Species. Trends Parasitol.; 32(8): 599–607.

[3] Gualdrón-López, M., Brennand, A., Hannaert, V., Quiñones, W., Cáceres, A.J., Bringaud, F., Concepción, J.L., Michels, P.A. (2012). When, how and why glycolysis became compartmentalized in the Kinetoplastea. A new look at an ancient organelle. Int J Parasitol.; 42(1): 1–20.

[4] Smith, T.K., Bringaud, F., Nolan, D.P., Figueiredo, L.M. (2017). Metabolic reprogramming during the Trypanosoma brucei life F1000Research, 6 (F1000 Faculty Rev):683 (https://doi.org/10.12688/f1000research.10342.2)

[5] Balogun, R.A. (1974). Studies on the amino acids of the tsetse fly, Glossina morsitans, maintained on in vitro and in vivo feeding systems. Comp Biochem Physiol A Comp Physiol.; 49(2A): 215–22.

[6] Herman, M., Pérez-Morga, D., Schtickzelle, N., Michels, P.A. (2008). Turnover of glycosomes during life-cycle differentiation of Trypanosoma brucei. Autophagy.; 4(3): 294–308.

[7] Hovel-Miner, G., Mugnier, M., Papavasiliou, F.N., Pinger, J., Schulz, D. (2015). A Host-Pathogen Interaction Reduced to First Principles: Antigenic Variation in T. brucei. Results Probl Cell Differ.; 57: 23–46.

[8] Nolan DP, Rolin S, Rodriguez, J.R., Van Den Abbeele, J., Pays, E. (2000). Slender and stumpy bloodstream forms of Trypanosoma brucei display a differential response to extracellular acidic and proteolytic stress. Eur J Biochem.; 267(1): 18–27.

[9] Clayton, C. (2019). Regulation of gene expression in trypanosomatids: living with polycistronic transcription. Open Biol. 9: 190072. http://dx.doi.org/10.1098/rsob.190072

[10] De Lange, T., Michels, P.A., Veerman, H.J., Cornelissen, A.W., Borst, P. (1984). Many trypanosome messenger RNAs share a common 50 terminal sequence. Nucleic Acids Res. 12, 3777–3790. (doi:10.1093/nar/12.9.3777)

[11] Koch, H., Raabe, M., Urlaub, H., Bindereif, A., Preusser, C. (2016). The polyadenylation complex of Trypanosoma brucei: characterization of the functional poly(A) polymerase. RNA Biol. 13, 221–231. (doi:10.1080/15476286.2015.1130208)

[12] Fadda, A., Färber, V., Droll, D., Clayton, C. (2013). The roles of 30-exoribonucleases and the exosome in trypanosome mRNA degradation. RNA (New York, N.Y.) 19, 937–947. (doi:10.1261/rna.038430.113)

[13] Kramer, S. (2017). The ApaH-like phosphatase TbALPH1 is the major mRNA decapping enzyme of trypanosomes. PLoS Pathog. 13, e1006456. (doi:10.1371/journal.ppat.1006456)

[14] Kolev, N., Franklin, J., Carmi, S., Shi, H., Michaeli, S., Tschudi, C. (2010). The transcriptome of the human pathogen Trypanosoma brucei at single-nucleotide resolution. PLoS Pathog. 6, e1001090. (doi:10.1371/journal.ppat.1001090)

[15] Siegel, T., Hekstra, D., Wang, X., Dewell, S., Cross, G. (2010). Genome-wide analysis of mRNA abundance in two life-cycle stages of Trypanosoma brucei and identification of splicing and polyadenylation sites. Nucleic Acids Res. 38, 4946–4957. (doi:10.1093/nar/gkq237)

[16] Peng, S.S., Chen, C.Y., Xu, N., Shyu, A.B. (1998). RNA stabilization by the AU-rich element binding protein, HuR, an ELAV protein. Embo. J., 17, 3461–3470.

[17] Peña-Diaz, P., Pelosi, L., Ebikeme, C., et al. (2012) Functional characterization of TbMCP5, a conserved and essential ADP/ATP carrier present in the mitochondrion of the human pathogen Trypanosoma brucei. J Biol Chem.; 287(50): 41861–74.

[18] St-Pierre, J., Brand, M.D., Boutilier, R.G. (2000). Mitochondria as ATP consumers: cellular treason in anoxia. Proc Natl Acad Sci U S A 97: 8670±8674. https://doi.org/10.1073/pnas.140093597 PMID: 10890886

[19] Pullman, M.E., Monroy, G.C. (1963). A Naturally Occurring Inhibitor of Mitochondrial Adenosine Triphosphatase. J Biol Chem 238: 3762±3769. PMID: 14109217

[20] Runswick, M.J., Bason, J.V., Montgomery, M.G., Robinson, G.C., Fearnley I.M., Walker J.E. (2013). The affinity purification and characterization of ATP synthase complexes from mitochondria. Open Biol.3120160 http://doi.org/10.1098/rsob.120160

[21] Panicucci, B., Gahura, O., Zíková, A. (2017). Trypanosoma brucei $TbIF_1$ inhibits the essential F1-ATPase in the infectious form of the parasite. PLoS Negl Trop Dis 11(4): e0005552. https://doi.org/10.1371/journal.pntd.0005552

[22] Vasquez, J., Hon, C., Vanselow, J., Schlosser, A., Siegel, T. (2014) Comparative ribosome profiling reveals extensive translational complexity in different Trypanosoma brucei life cycle stages. Nucleic Acids Research, Volume 42, Issue 6, Pages 3623–3637, https://doi.org/10.1093/nar/gkt1386

[23] Gahura, O., Šubrtová, K., Váchová, H., Panicucci, B., Fearnley, I.M., Harbour, M.E., Walker, J.E. and Zíková, A. (2018). The F1-ATPase from Trypanosoma brucei is elaborated by three copies of an additional p18-subunit. FEBS J, 285: 614-628. doi:10.1111/febs.14364

[24] Quijada, L. et al. (2002). Expression of the human RNA-binding protein HuR in Trypanosoma brucei increases the abundance of mRNAs containing AU-rich regulatory elements. Nucleic Acids Research, Volume 30, Issue 20, Pages 4414–4424 https://doi.org/10.1093/nar/gkf577

[25] Gruber, A.R., Lorenz, R., Bernhart, S.H., Neuböck, R., Hofacker, I.L. (2008). The Vienna RNA Websuite., Nucleic Acids Research, Volume 36, Issue suppl_2, Pages W70–W74, https://doi.org/10.1093/nar/gkn188

[26] Hehl, A., Vassella, E., Braun, R. and Roditi, I. (1994). A conserved stem-loop structure in the 3' untranslated region of procyclin mRNAs regulates expression in Trypanosoma brucei. PNAS January 4, 1994 91 (1) 370-374; https://doi.org/10.1073/pnas.91.1.370

[27] Furger, A. et al. (1997). Elements in the 3' untranslated region of procyclin mRNA regulate expression in insect forms of Trypanosoma brucei by modulating RNA stability and translation. Molecular and Cellular Biology 17.8: 4372-4380. Web. 23 Dec. 2019.

[28] Mayho, M., Fenn, K., Craddy, P., Crosthwaite, S., Matthews, K. (2006) Post-transcriptional control of nuclear-encoded cytochrome oxidase subunits in Trypanosoma brucei: evidence for genome-wide conservation of life-cycle stage-specific regulatory

elements, Nucleic Acids Research, Volume 34, Issue 18, Pages 5312–5324, https://doi.org/10.1093/nar/gkl598

[29] Mugo, E., Clayton, C. (2017). Expression of the RNA-binding protein RBP10 promotes the bloodstream-form differentiation state in Trypanosoma brucei. PLoS Pathog 13(8): e1006560. https://doi.org/10.1371/journal.ppat.1006560

[30] Najafabadi, H., Lu, Z., MacPherson, C., Mehta, V., Adoue, V., Pastinen, T., Salavati, R. (2013). Global identification of conserved post-transcriptional regulatory programs in trypanosomatids, Nucleic Acids Research, 2013, Vol. 41, No. 18 8591–8600 doi:10.1093/nar/gkt647

[31] Wurst, M., Seliger, B., Jha, B., Klein, C., Queiroz, R., and Clayton, C. (2012). Expression of the RNA recognition motif protein RBP10 promotes a bloodstream-form transcript pattern in Trypanosoma brucei. Molecular Biology 83(5), 1048-1063. Doi:10.1111/j.1365-2958.2012.07988.x

[32] Dejung, M., Subota, I., Bucerius, F., Dindar, G., Freiwald, A., Engstler, M., et al. (2016). Quantitative proteomics uncovers novel factors involved in developmental differentiation of Trypanosoma brucei. PLoS Pathog.; 12(2):e1005439. Epub 2016/02/26. https://doi.org/10.1371/journal.ppat.1005439 PMID: 26910529

[33] Kolev, G., Ramey-Butler, K., Cross, G., Ullu, E., Tschudi, C. (2012). Developmental Progression to Infectivity in Trypanosoma brucei Triggered by an RNA-Binding. Science 338 (6112), 1352-1353. DOI: 10.1126/science.1229641

[34] Beta tubulin genes of T. brucei (2019, December 22). Retrieved from https://www.ncbi.nlm.nih.gov/genome/gdv/?org=trypanosoma-brucei

[35] Merk. (2019). GenElute™ Mammalian Genomic DNA Miniprep Kit Protocol: manual. Darmstadt: Merk

[36] gDNA extraction scheme (2019, June 10). Retrieved from: https://www.sigmaaldrich.com/technical-documents/protocols/biology/genelute-mammalian-genomic-dna-miniprep-kit.html

[37] Thermo Fisher Scientific. (2019). Invitrogen™ TURBO DNA-free™ Kit: manual. Waltham: Thermo Fisher Scientific.

[38] New England Biolabs. (2019). DNase I (RNase-free): manual. Ipswich: New England Biolabs

[39] Thermo Fisher Scientific. (2019). Invitrogen™ TaqMan™ Reverse Transcription Reagents: manual. Waltham: Thermo Fisher Scientific.

[40] Roche. (2015). LightCycler® 480 SYBR Green I Master: manual. Basel: Roche

[41] ELISA schematic. (2019, June 10). Retrieved from: https://www.researchgate.net/figure/Principle-for-sandwich-ELISA-detecting-CAT-enzyme-The-ELISA-plate-is-coated-with_fig1_44392133

[42] Merk. (2019). CAT ELISA: product manual. Darmstadt: Merk

[43] Thermo Fisher Scientific. (2019). Pierce™ BCA Protein Assay Kit: manual. Waltham: Thermo Fisher Scientific

[44] Colasante, C., Robles, A., Li, C.-H., Schwede, A., Benz, C., Voncken, F., Clayton, C. et al. (2007). Regulated expression of glycosomal phosphoglycerate kinase in Trypanosoma brucei. Molecular and Biochemical Parasitology, 151(2), 193–204. doi:10.1016/j.molbiopara.2006.11.003

[45] Schenborn, E., Groskreutz, D. (1999). Reporter gene vectors and assays. Mol Biotechnol 13, 29–44. https://doi.org/10.1385/MB:13:1:29

[46] Droll, D., Minia, I., Fadda, A., Singh, A., Stewart, M., et al. (2013) Post-Transcriptional Regulation of the Trypanosome Heat Shock Response by a Zinc Finger. Protein. PLoS Pathog 9(4): e1003286. doi:10.1371/journal.ppat.1003286

[47] Jojic, B., Amodeo, S., Bregy, I., & Ochsenreiter, T. (2018). Distinct 3' UTRs regulate the life-cycle-specific expression of two TCTP paralogs in Trypanosoma brucei. Journal of cell science, 131(9), jcs206417. https://doi.org/10.1242/jcs.206417

[48] Neumann, J. et al. (1987). A novel rapid assay for chloramphenicol acetyltransferase gene expression. Biotechniques 5,444-448

[49] Abken, H. and Reifenrath, B. (1992). A procedure to standardize CAT reporter gene assay. Nucleic Acids Res. 1992 Jul 11; 20(13): 3527. doi: 10.1093/nar/20.13.3527

[50] Chloramphenicol Acetyltransferase Gene in E. coli (2020, March 17). Retrieved from https://www.ncbi.nlm.nih.gov/gene/2847485

[51] Schneider-Poetsch, T., Ju, J., Eyler, D.E., Dang, Y., Bhat, S., Merrick, W.C., Green, R., Shen, Ben., Liu, J.O. (2010). Inhibition of Eukaryotic Translation Elongation by Cycloheximide and Lactimidomycin. Nat Chem Biol. 2010 Mar; 6(3): 209–217. (doi: 10.1038/nchembio.30)

[52] Romaniuk, M. A., Frasch, A. C., & Cassola, A. (2018). Translational repression by an RNA-binding protein promotes differentiation to infective forms in *Trypanosoma cruzi*. PLoS pathogens, 14(6), e1007059. https://doi.org/10.1371/journal.ppat.1007059

[53] Kumar Gupta, S., Kosti, I., Plaut, G., Pivko, A., Tkacz, I.D., Cohen-Chalamish, S., Kumar Biswas, D., Wachtel, C., Ben-Asher, H.W., Carmi, S., Glaser, F., Mandel-Gutfreund, Y., Michaeli, S. (2013) The hnRNP F/H homologue of Trypanosoma brucei is differentially expressed in the two life cycle stages of the parasite and regulates splicing and mRNA stability, Nucleic Acids Research, Volume 41, Issue 13, Pages 6577–6594, https://doi.org/10.1093/nar/gkt369

[54] Singh, A., Minia, I., Droll, D., Fadda, A., Clayton, C., Erben, E. (2014). Trypanosome MKT1 and the RNA-binding protein ZC3H11: interactions and potential roles in post-transcriptional regulatory networks, Nucleic Acids Research, Volume 42, Issue 7, Pages 4652–4668, https://doi.org/10.1093/nar/gkt1416

[55] Imboden, M., Blum, B., DeLange, T., Braun, R., Seebeck, T. (1986). Tubulin mRNAs of Trypanosoma brucei. Journal of Molecular Biology. Volume 188, Issue 3, Pages 393-402, ISSN 0022-2836. Doi: https://doi.org/10.1016/0022-2836(86)90163-4.

[56] Butter, F., Bucerius, F., Michel, M., Cicova, Z., Mann, M., Janzen, C.J. (2012). Comparative Proteomics of Two Life Cycle Stages of Stable Isotope-labeled Trypanosoma brucei Reveals Novel Components of the Parasite's Host Adaptation Machinery. Molecular & Cellular Proteomics,12 (1) 172-179; DOI:10.1074/mcp.M112.019224

[57] Mulindwa, J., Mercé, C., Matovu, E. et al. (2015). Transcriptomes of newly-isolated Trypanosoma brucei rhodesiense reveal hundreds of mRNAs that are co-regulated with stumpy-form markers. BMC Genomics 16, 1118 https://doi.org/10.1186/s12864-015-2338-y

[58] Erben, E.D., Fadda, A., Lueong, S., Hoheisel, J.D., Clayton, C. (2014). A genome-wide tethering screen reveals novel potential post-transcriptional regulators in

Trypanosoma brucei. PLoS pathogens, 10(6), e1004178. https://doi.org/10.1371/journal.ppat.1004178

[59] Kramer, S., Queiroz, R., Ellis, L., Hoheisel, J.D., Clayton, C., Carrington, M. (2010) The RNA helicase DHH1 is central to the correct expression of many developmentally regulated mRNAs in trypanosomes. Journal of Cell Science 123: 699-711; doi: 10.1242/jcs.058511

[60] Ingolia, N. T., Ghaemmaghami, S., Newman, J. R., Weissman, J. S. (2009). Genome-wide analysis in vivo of translation with nucleotide resolution using ribosome profiling. Science (New York, N.Y.), 324(5924), 218–223. https://doi.org/10.1126/science.1168978

[61] Andreev, D.E., O'Connor, P.F., Loughran, G., Dmitriev, S.E., Baranov P.V., Shatsky I.N. (2017). Insights into the mechanisms of eukaryotic translation gained with ribosome profiling, Nucleic Acids Research, Volume 45, Issue 2, Pages 513–526, https://doi.org/10.1093/nar/gkw1190

[62] Ingolia N.T., Lareau L.F., Weissman J.S. (2011). Ribosome profiling of mouse embryonic stem cells reveals the complexity and dynamics of mammalian proteomes. Cell.; 147:789–802.

[63] Dunn J.G., Foo C.K., Belletier N.G., Gavis E.R., Weissman J.S.. (2013). Ribosome profiling reveals pervasive and regulated stop codon readthrough in Drosophila melanogaster. eLife. 2:e01179.

[64] Parsons, M., Ramasamy, G., Vasconcelos, E. J., Jensen, B. C., Myler, P. J. (2015). Advancing Trypanosoma brucei genome annotation through ribosome profiling and spliced leader mapping. Molecular and biochemical parasitology, 202(2), 1–10. https://doi.org/10.1016/j.molbiopara.2015.09.002

[65] Kasari, V., Margus, T., Atkinson, G.C. et al. Ribosome profiling analysis of eEF3-depleted Saccharomyces cerevisiae. Sci Rep 9, 3037 (2019). https://doi.org/10.1038/s41598-019-39403-y

[66] Batey R. T. (2014). Advances in methods for native expression and purification of RNA for structural studies. Current opinion in structural biology, 26, 1–8. https://doi.org/10.1016/j.sbi.2014.01.014

8. Appendices

Appendix 1: Sequence of $TbIF_1$ 3'UTR:

The 3' UTR of $TbIF_1$ contains various possible regulatory sites. The elements are marked in the sequence.

GAAGGAGCAG*GCGTCATTCGC*AAGAGCTCTACCACAA*TGTTAACAAACATGTA*AAACCG
CCA*TTATATATATATATATATATATATAA*GCAACGAGCGTAACG**TTTTTTCTTT**AGCTAAAAT
GGTCTCAATTTCCTATAAAACG**TTTCTTTTTTTTTTTT**CACCTCCAAAATATTATCACT
ACTGTGACAAATCATGAAAACTGCTATTATTGT**TATTTTTT**ATTTATTACTTCTTCATT
TCCACTCAAAATAA**TATTTTTT**CATGCACTTTCCATCAGTTGCAACCCTTCCTCACCAT
GTCACACCAAAACGGCCACCACTCCAACAAGGTTTTCTATTCGGGTCACTGTGGAACT
ACGAATCCGACACAACTGGGGCAGCACGTGGCAGGACCAAGTGAAAGGCAACGCGTG
CATTGAAACAGTGCTTGATGTGGGCCTCTTGATATTTGTCTGCAG

ATGC	Predicted secondary structures
TTTT	U-rich elements – involved in the regulation of PF-specific genes
TATTTTTT	Rbp10 binding motif
ATTTATT	Rbp6 binding motif

Appendix 2: Hetero-distributed variances of the CAT reporter mRNA levels

Reporter variant	**1-457**	**91-457**	**192-457**	**267-457**	**ΔRbp6/10_1,2**	**ΔRbp10_1,2**	**ΔRbp10_1**	**ΔRbp10_2**	**ΔRbp6**	**ΔRbp6/10_1**	**ACT**
variance	0.02	0.03	0.43	1.04	0.25	0.00	0.44	0.80	0.19	0.04	0.17

Appendix 3: Hetero-distributed variances of the reporter protein levels

Reporter variant	**1-457**	**91-457**	**192-457**	**267-457**	**ΔRbp6/10_1,2**	**ΔRbp10_1,2**	**ΔRbp10_1**	**ΔRbp10_2**	**ΔRbp6**	**ΔRbp6/10_1**	**ACT**
variance	0.01	0.17	0.00	5.20	0.02	5.71	1.53	0.33	0.16	0.00	1.65